Calcified metazoans in thrombolite-stromatolite reefs of the terminal Proterozoic Nama Group, Namibia

John P. Grotzinger, Wesley A. Watters, and Andrew H. Knoll

Abstract.—Reefs containing abundant calcified metazoans occur at several stratigraphic levels within carbonate platforms of the terminal Proterozoic Nama Group, central and southern Namibia. The reef-bearing strata span an interval ranging from approximately 550 Ma to 543 Ma. The reefs are composed of thrombolites (clotted internal texture) and stromatolites (laminated internal texture) that form laterally continuous biostromes, isolated patch reefs, and isolated pinnacle reefs ranging in scale from a meter to several kilometers in width. Stromatolite-dominated reefs occur in depositionally updip positions within carbonate ramps, whereas thrombolite-dominated reefs occur broadly across the ramp profile and are well developed as pinnacle reefs in downdip positions.

The three-dimensional morphology of reef-associated fossils was reconstructed by computer, based on digitized images of sections taken at 25-micron intervals through 15 fossil specimens and additionally supported by observations of over 90 sets of serial sections. Most variation observed in outcrop can be accounted for by a single species of cm-scale, lightly calcified goblet-shaped fossils herein described as *Namacalathus hermanastes* gen. et sp. nov. These fossils are characterized by a hollow stem open at both ends attached to a broadly spheroidal cup marked by a circular opening with a downturned lip and six (or seven) side holes interpreted as diagenetic features of underlying biological structure. The goblets lived atop the rough topography created by ecologically complex microbial-algal carpets; they appear to have been sessile benthos attached either to the biohermal substrate or to soft-bodied macrobenthos such as seaweeds that grew on the reef surface. The phylogenetic affinities of *Namacalathus* are uncertain, although preserved morphology is consistent with a cnidarian-like bodyplan. In general aspect, these fossils resemble some of the unmineralized, radially symmetric taxa found in contemporaneous sandstones and shales, but do not appear to be closely related to the well-skeletonized bilaterian animals that radiated in younger oceans. Nama reefs demonstrate that biohermal associations of invertebrates and thrombolite-forming microorganisms antedate the Cambrian Period.

John P. Grotzinger and Wesley A. Watters.   Department of Earth, Atmospheric and Planetary Sciences, Massachusetts Institute of Technology, Cambridge, Massachusetts 02139. E-mail: grotz@mit.edu and E-mail: watters@mit.edu

Andrew H. Knoll.   Botanical Museum, Harvard University, Cambridge, Massachusetts 02138. E-mail: aknoll@oeb.harvard.edu

Introduction

Siliciclastic successions of terminal Proterozoic age contain moderately diverse, commonly problematic fossils of soft-bodied organisms, collectively known as the Ediacaran biota. Many rocks that host Ediacaran assemblages also contain a limited diversity of metazoan trace fossils. In contrast—and in strong contradistinction to Cambrian and younger successions—terminal Proterozoic limestones have been thought to yield only limited evidence of animal life. A major exception to this pattern is provided by *Cloudina,* a globally distributed calcified fossil known almost exclusively from uppermost Proterozoic carbonate rocks. But should *Cloudina* be regarded as the exception that proves the rule or as a hint that more diverse animals inhabited carbonate platforms before the dawn of the Cambrian?

Here, we report evidence for a paleoecologically distinctive assemblage of calcified metazoans in thrombolite-stromatolite reefs and associated facies of the terminal Proterozoic Nama Group, Namibia, where *Cloudina* was originally discovered. Particularly abundant are goblet-shaped fossils described in this paper as *Namacalathus hermanastes* gen. et sp. nov., and interpreted as lightly mineralized, attached benthos comparable to simple cnidarians in bodyplan.

Archaeocyathans and corallimorph metazoans formed persistent ecological associa-
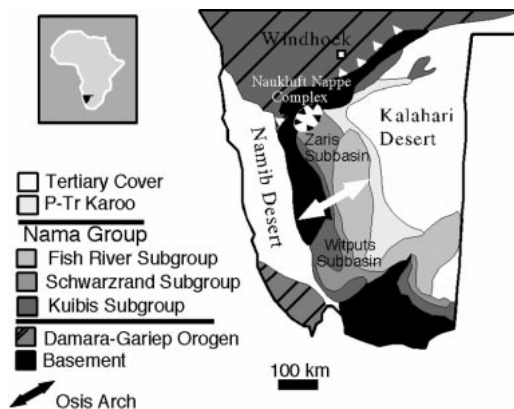
FIGURE 1.   Geological map of southern Namibia, showing the distribution of major sedimentary and tectonic elements, including the Nama Group, discussed in the text.

tions with microbial communities in Early (but not earliest) Cambrian reefs (e.g., Riding and Zhuravlev 1995), and stromatolite-thrombolite reefs have been reported from upper (but not uppermost) Proterozoic successions (e.g., Turner et al. 1993, 2000). Therefore, in addition to contributing evidence of diversity among terminal Proterozoic skeletons, the fossiliferous bioherms reported here help to fill a gap in our understanding of the sedimentary transition from Proterozoic reefs accreted by physical and microbial processes to Phanerozoic structures in which mineralized algae and animals play important constructional roles.

Geological Setting of Nama Reefs

The geology of southern Namibia, including the distribution of the Nama Group, is shown in Figure 1. The Nama Group has been interpreted as a foreland basin fill (Germs 1983; Gresse and Germs 1993) related to convergence along the western and northern margins of the Kalahari craton and overthrusting in the Gariep and Damara orogens (Miller 1983). The general stratigraphy of the Nama Group (Fig. 2) was outlined by Martin (1965) and developed in a series of papers by Germs (1972, 1974, 1983). Regional isopachs and facies distributions define two subbasins; the Witputs subbasin, located in southern Namibia, thickens toward the Gariep orogenic belt, while the more northerly Zaris subbasin

thickens northward toward the Damara orogenic belt. The Osis Arch represents a site of depositional thinning of all Nama units that separates the two subbasins (Fig. 1).

In general, the Nama Group consists of a number of marine-shelf siliciclastic and carbonate sequences (Kuibis and Schwarzrand Subgroups) overlain by alluvial to shallow marine molasse (Fish River Subgroup) that documents unroofing of the Damara/Gariep hinterlands. Near the subbasin axes, thicknesses are on the order of 2–3 km, thinning to less than 1 km farther onto the craton toward the Osis Arch (Germs 1974, 1983). Thrombolite-stromatolite reefs are well developed in the Kuibis Subgroup of the northern, Zaris subbasin, and in the Huns platform of the southern, Witputs subbasin (Fig. 2).

Geochronologic constraints (Grotzinger et al. 1995) are provided by U-Pb zircon ages on several units within the Nama Group (Fig. 2). An ash bed within the northern Nama basin yields an age of 548.8 $\pm$ 1 Ma for the middle Kuibis Subgroup (Grotzinger et al. 1995). In southern exposures of the Nama, the overlying Schwarzrand Subgroup contains ash beds that yield, in ascending order, ages of 545.1 Ma, 543.3 Ma, and 539.4 Ma (all $\pm$1 Ma) (Grotzinger et al. 1995). The Proterozoic/Cambrian boundary in Namibia is bracketed by the 543.3 Ma and 539.4 Ma ages, although this also includes a significant unconformity; on a global basis the Proterozoic/Cambrian boundary is currently regarded to be on the order of 543 Ma.

Zaris Subbasin—Kuibis Platform

The basal unit of the Nama Group, the Kuibis Subgroup is regionally widespread, consisting of a thin, basal, transgressive sandstone that grades upward into a carbonate platform 150–500 m thick (Figs. 2, 3A). In the Zaris subbasin, Kuibis rocks form a well-developed carbonate ramp that thickens from the Osis Arch northward to the Naukluft Mountains (Germs 1983; Saylor et al. 1998; Smith 1998). This change in thickness is accompanied by a gradation from shallow-water facies in the south to deeper-water, basinal facies near the Naukluft Mountains (Germs 1983). Germs (1972b, 1974, 1983) subdivided
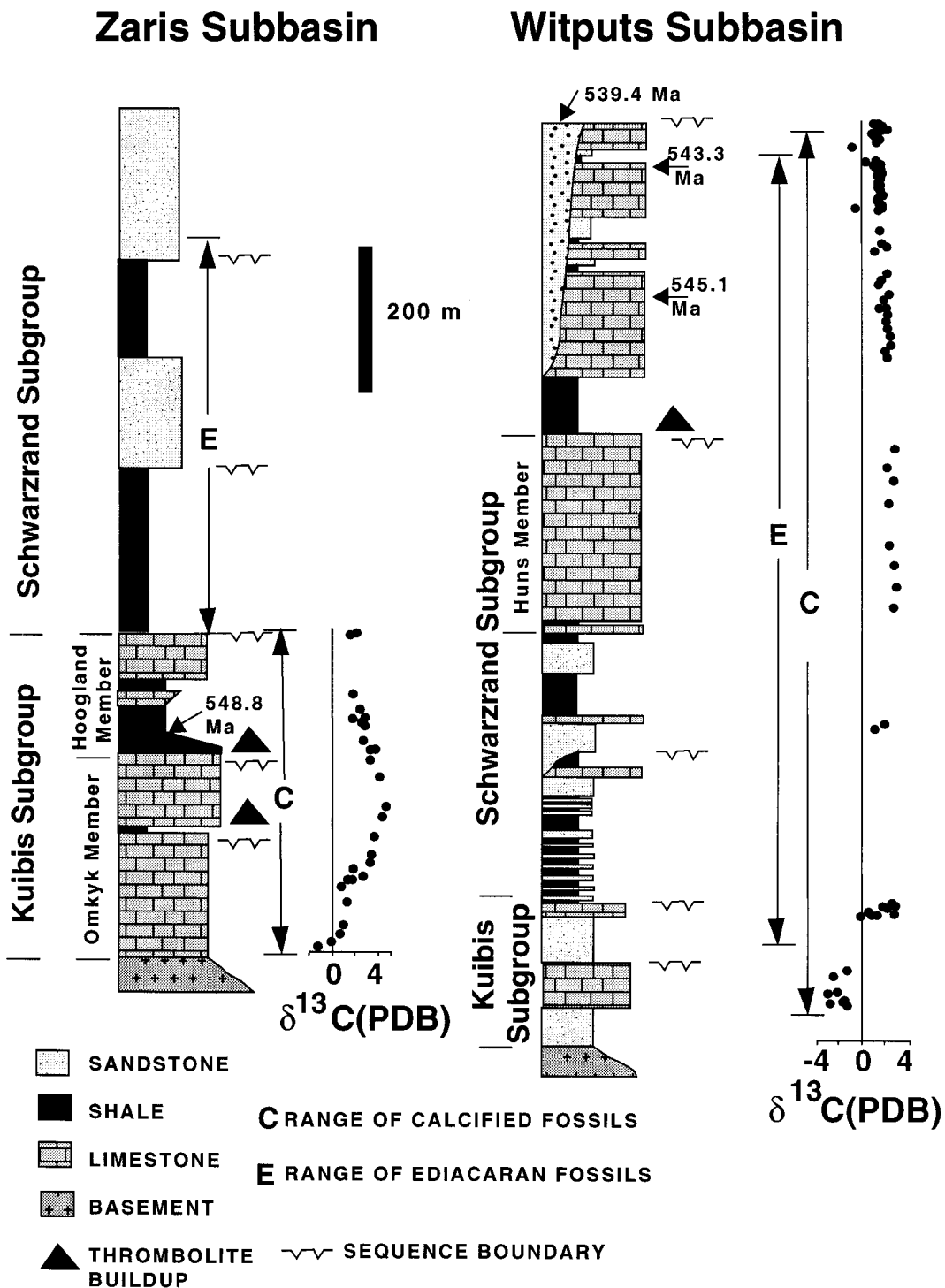
FIGURE 2.   Generalized stratigraphy of the Nama Group for the Zaris (north) and Witputs (south) subbasins, show-ing major lithostratigraphic, chemostratigraphic, biostratigraphic, and sequence stratigraphic attributes. Note the positions of thrombolite reef complexes above sequence boundaries.

the Kuibis platform into two members (Omkyk and Hoogland; Fig. 2) that correspond approximately to stratigraphic sequences (Grotzinger et al. 1995; Saylor et al. 1995, 1998; Smith 1998). The surfaces defining the member boundaries, however, represent flooding events rather than sequence boundaries (Smith 1998). Detailed mapping of these sequences (Smith 1998) shows that the reefs described here, including the Driedoornvlagte bioherm identified by Germs (1972a, 1974), all nucleated within the Transgressive Systems to early Highstand Systems Tract (TST to HST) at the base of their respective sequences (Fig. 2). This implies that the most favorable conditions for reef growth occurred during times of increased accommodation and lowered sediment flux on the platform, similar to reefs of older Proterozoic (Grotzinger 1989; Grotzinger and James 2000) and Phanerozoic age (Soreghan and Giles 1999).

In updip sections, biostromes form continuous sheets (within the Zebra River farm) that break up into patch-reef bioherms toward and within the Donkergange farm (Fig. 3B,C). Further downdip, large pinnacle reefs are developed at Driedoornvlagte in a position of maximum accommodation within the depositional profile (Fig. 3A).

Witputs Subbasin—Huns Platform

The Huns Member consists of a thick section (up to 500 m) of platform carbonates in the middle of the Nama Group, within the Witputs subbasin of southern Namibia (Fig. 2). Germs (1972b, 1974, 1983) first recognized pinnacle reefs on the Swartkloofberg farm; subsequent work (Grotzinger et al. 1995; Saylor and Grotzinger 1996; Saylor et al. 1998) has shown that these reefs are associated with drowning of the platform. Fifty to 70 m wide at their base and up to 50 m high (Fig. 4), Huns reefs are blanketed by shales deposited at or below wave base.

Facies and Diagenesis

The thrombolite biostrome facies consists of massive thrombolites, stratiform thrombolites and stromatolitic thrombolite-forming columns, branching columns, and heads and domes of decimeter-scale dimensions and relief (Fig. 5A). In general, the cores of domes and columns are characterized by a thrombolitic texture, whereas the margins become progressively more stromatolitic in nature, in the sense that they exhibit crude lamination (Fig. 5A; equivalent to the stromatolitic thrombolites of Kennard and James 1986). In the Kuibis reefs, columns are consistently elongated with an azimuth of 270°–310°. Calcified macrofossils occur within thrombolite domes and columns, and the intrachannel fill between domes and columns consists of trough cross-bedded, fossiliferous packstone and grainstone containing simple tubes, more complex cups and goblets, and their bioclastic detritus (Fig. 5A). Figure 7 shows the close relationship between fossil content and thrombolitic texture.

The thrombolite biostrome facies characteristically developed as broad, laterally continuous reef complexes that became discontinuous down depositional dip to form isolated bioherms and pinnacle reefs. Energy conditions were high, as demonstrated by the trough cross-bedded intrachannel grainstone, the elongation of the stromatolitic thrombolite columns, and the association of this facies with the grainstone facies. The consistent orientation of the thrombolite elongation is comparable to that of other platforms where wave action is inferred to have been responsible for the elongation of stromatolites (Hoffman 1969; Cecile and Campbell 1978; Grotzinger 1986; Bartley et al. 1998), analogous to the development of "spur and groove" structure in modern coral reefs. This interpretation supports other evidence that the Kuibis ramp was a wave- and storm-dominated system, where the dominant currents were induced by strong wave-generated flows.

The internal texture of the thrombolite reefs is characterized by mesoclots that range from a few millimeters to a few centimeters in diameter (Figs. 5A,B, 6). Nama mesoclots are restricted to simple ovoid, globose, and colliform morphologies and do not include the complex digitate or dendriform fabrics found in younger thrombolites (e.g., Kennard and James 1986; Riding and Zhuralev 1995). Nama mesoclots formed an open framework that resulted in development of abundant cavities
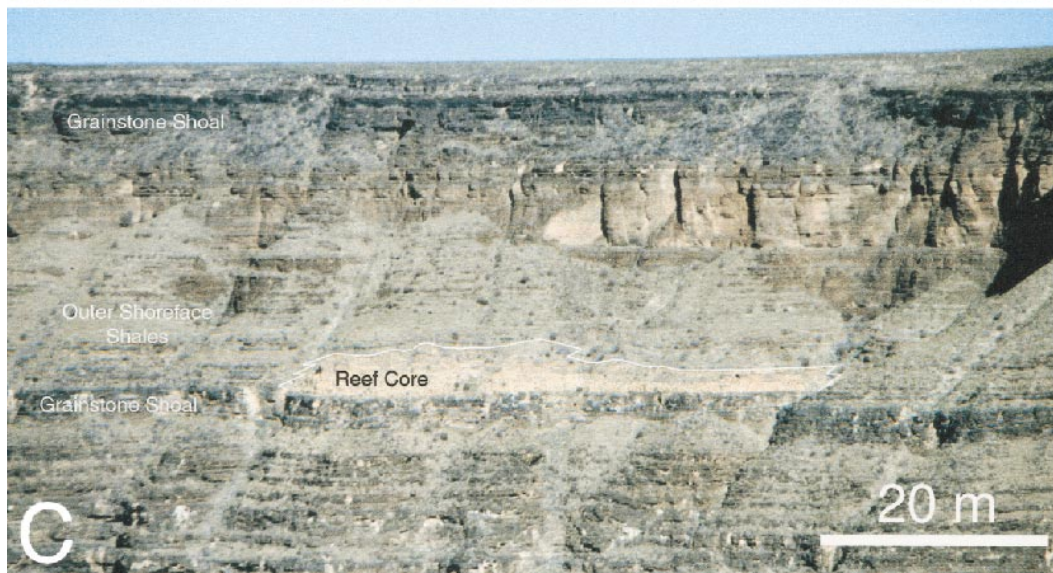
(Figs. 5B, 6). Mesoclots typically were overgrown by a synsedimentary crust of fibrous marine cement that now consists of calcite but is interpreted to have replaced original aragonite (Fig. 6). Marine cement crusts were subsequently covered by geopetal sediment, which partially filled framework pores (Fig. 5B, 6). Remaining porosity was occluded by a dolomite rim cement, followed by infilling with blocky calcite spar (Fig. 6). Recrystallization commonly makes interpretation of growth processes difficult, but sporadically distributed patches with relatively good fabric preservation show evidence that coccoidal microorganisms, expressed as poorly preserved spheroids in mesoclot cores, contributed to reef accretion (Grotzinger in press).

Early lithification of thrombolites and stromatolites in Nama pinnacle reefs resulted in the development of penetrative networks of neptunian dikes (Fig. 5C). These are best expressed in the Huns reefs and Driedoornvlagte bioherm, where fractures that cut sharply across reefs are filled with fibrous marine cements, interpreted as calcite-replaced aragonite (Fig. 5C). Neptunian dikes are formed only in the larger reefs, where gravitationally induced failure of the reef was likely. A related effect includes failure of the sides of the pinnacle reefs, which resulted in down-slope transport of slide breccias. These breccias are composed of angular blocks up to one meter in diameter with thrombolite and stromatolite textures. Voids between breccia blocks are filled with massive lime or dolomite mudstones, or fibrous marine cements.

Calcified Metazoans of the Nama Group

Within thrombolitic facies, fossils occur abundantly both in the domal and columnar structures that make up individual reefs and in trough cross-bedded intrachannel fill. The fossils—millimeter- to centimeter-scale calcareous cups, goblets, and tubes—are particularly abundant in thrombolites and thrombolitic stromatolites, evidently preferring the firm substrate and bathymetric elevation that these structures offered (Fig. 7). Intrachannel fill consists of skeletal packstone and grainstone containing goblets, cups, cylindrical tubes, *Cloudina,* and their bioclastic detritus.

Morphology.—Figure 8 shows a number of calcified goblet-shaped fossils. Two dimensional slices provided by outcrops, polished slabs, and thin-sections reveal a moderate degree of assemblage variability, ranging from clearly defined goblet-shaped forms (Fig. 8E, originally illustrated in Grotzinger et al. 1995), to rounded cups without ''stems,'' to bulbous structures showing apparent hexagonal symmetry in cross-section.

Exposed specimens reflect some combination of intraspecific, interspecific, and taphonomic variation, but the relative contributions of these factors cannot be evaluated in the absence of information about the three-dimensional morphology of constituent fossils. Because the fossils are preserved as calcitic void-fill in a calcite matrix, individual specimens cannot be freed by conventional techniques—posing a challenge for morphological and, hence, systematic interpretation. Our response has been to develop a computer-based, ''tomographic'' reconstruction technique to de-

←

FIGURE 3.   Reefs of the Zaris subbasin. A, Landsat TM image showing pinnacle reef (Driedoornvlagte bioherm) on the Driedoornvlagte farm, Zaris subbasin. The reef is developed on platform carbonates (dark-blue colors) and is overlain by deep-water shales (orange-red colors). The platform carbonates unconformably overlie much older quartzites (mauve-gray colors at top of photograph). A road runs along Quaternary alluvium (white, cream colors) that covers the stratigraphically lowest shales. Color in the TM image indicates composition—the reef has a gray-lavender color that reflects high dolomite content, whereas the dark-blue color of shallow-water platform carbonates reflects dominance of limestone. Rocks have a structural dip of about 40° toward the south. B, Laterally continuous biostrome at the top of the Omkyk Member within Donkergange passes laterally into discrete patch reefs, each indicated by an ''R.'' Reefs are overlain by deep-water shales, which in turn pass upward into a grainstone shoal complex. C, Close-up of a representative patch reef showing stratigraphic position immediately above a sequence boundary, which separates reef facies from underlying thick-bedded grainstone facies. The reef passes laterally into relatively thin-bedded shales and fine calcarenites. Note how bedding thickness decreases immediately above the sequence boundary, indicating a regime of increasing accommodation.
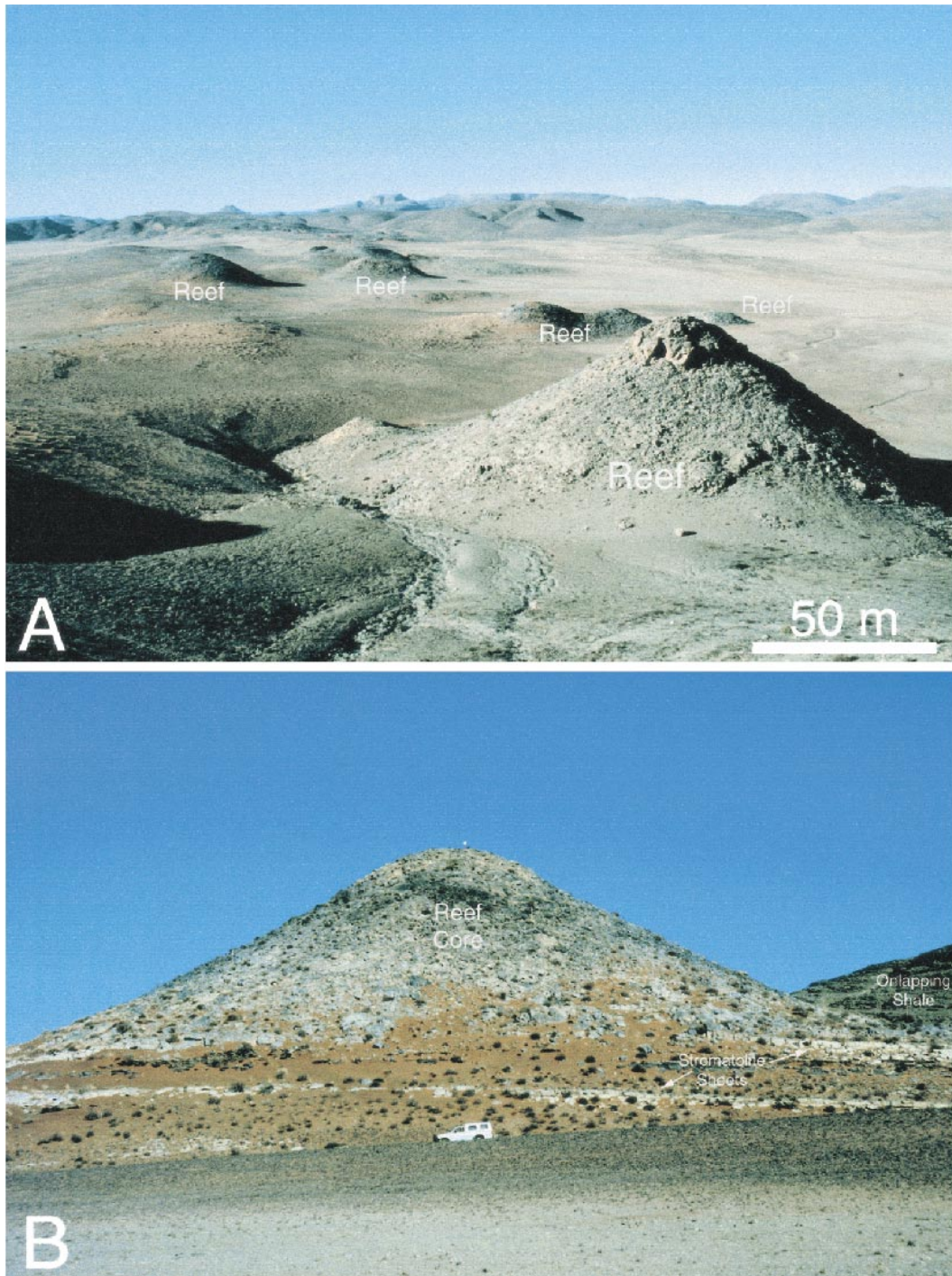
FIGURE 4.   Thrombolite-stromatolite pinnacle reefs at top of Huns platform, Witputs subbasin, southern Namibia. Reefs are formed of a core of coalesced thrombolite mounds, overgrown by a stromatolitic mantle. A, Overview of multiple pinnacle reefs formed at top of Huns platform. Reefs have been exhumed by erosion of overlying shales. B, Cross-section of representative pinnacle reef showing its foundation of stromatolite sheet facies and remnants of overlying shales that have been eroded to expose reefs. A sequence boundary separates the stromatolite sheet- and pinnacle reef facies; thus, the pinnacle reefs formed during a time of increasing accommodation space within a Transgressive System Tract.

termine their true three-dimensional geometry.

In brief, appropriate samples were selected, the position of each sample and its contained fossils calibrated with respect to an external reference system, 25 μ ground from the polished sample surface, and the ground surface photographed using a digital camera. In this study, the last two steps were iterated several hundred times for samples taken from reefs at Vioolsdrift (Witputs subbasin) and Donkergange (Zaris subbasin). Contours of the fossils in each cross-sectional image were obtained using a battery of image-processing techniques, including a binary thresholding procedure. Ultimately, the three-dimensional surface of our models is determined by the shape of these contours, placed adjacent to one another in the third dimension and connected using Delaunay triangulation to interpolate the surface points between contour layers. In this process, segments in a given contour layer are connected to the vertices in an adjacent layer, ultimately allowing the complete surface to be described by a set of triangular tiles. Multiple views of one complete and eight partial tomographic reconstructions are shown in Figure 9. Additional morphological data are provided by six additional reconstructions and more than 90 sets of serial sections not used in generating reconstructions. (A detailed description of the digital reconstruction technique used here is presented in Watters 2000 and Watters and Grotzinger in press.)

All complete or nearly complete reconstructed specimens have a stem and an outward-flaring cup. The cup, a few millimeters to 2.5 cm in maximum dimension, has a broad circular opening at the top with a lip that curves inward. The cup is perforated by six or seven holes of similar size and shape and has a matching number of regularly arranged side walls. Cups taper to a shallow base from which a hollow cylindrical stem extends. Some specimens contain an additional hole near the cup base. Stems are commonly longer than maximum cup dimension and are open at both ends.

In constructing a model morphology from reconstructed individuals, we took note of variation in the following parameters: (1) the radial profile of the cup; (2) the aspect ratio of the cup (i.e., maximum diameter to total height); (3) the size and shape of the cup's inner lip; (4) the relative size of the cup's circular opening; (5) the curvature of cup walls (wall curvature varies with height, in some cases flattening midway up the cup wall and in others remaining rounded); (6) the size, shape, and position of holes (e.g., oval or circular, located at the top, middle, or base of the cup; and with or without an inward-turning lip); (7) the thickness of walls; (8) the number of sides and holes (i.e., six or seven); (9) the length of the stem; (10) the size of the cup; and (11) the trajectory and radial profile of the stem.

In developing a mathematical model for the morphology of these fossils, only the features listed above were assumed. Individual tomographic reconstructions were used to obtain values for all 11 parameters, enabling us to generate individual models. Figures 10A and 10C show sample cross-sections of tomographic reconstructions that were used to measure profiles of the cup's radius and inward lip, the cup's aspect ratio, and the number of holes and side-wall sections. The corresponding mathematical models are shown in Figures 10B and 10D.

An exhaustive database of randomly oriented synthetic cross-sections was obtained from the models depicted in Figure 10. These synthetic cross-sections reproduce the vast majority of shapes observed in rocks, a subset of which is depicted in Figure 11. Because we can account for most observed variation by a combination of random sections through the morphologies reconstructed in Figure 10 and simple taphonomic alterations (e.g., physical distortion) observed in our samples, we interpret most of the variation seen in outcrop as representing a single species population. Figure 12 illustrates the variation in cup size (maximum diameter) and shape (aspect ratio = maximum diameter/height) for a sample population of reconstructed specimens from a single rock sample.

Mineralization.—*Cloudina* was only lightly mineralized, apparently by the precipitation of calcite in an organic template (Grant 1990). The same is true of the new taxon, *Namacala-*

thus hermanastes, reported here. Like *Cloudina, Namacalathus* had thin walls (little more than 100 m thick in best-preserved specimens) that deformed flexibly during compaction (Fig. 13). Petrographically, most fossils are preserved as casts of void-filling calcite, with rare evidence of thin, organic-rich wall structures (Fig. 13D–F). Such fossils might be interpreted as casts and molds of unmineralized organisms, were it not for fragmental remains that were almost certainly mineralized before fracture and dispersal. Original carbonate mineralogy is difficult to determine because of extensive dissolution or replacement, but common overgrowth of shells by euhedral calcite crystals supports the interpretation of a calcite precursor for *Namacalathus.* Overgrowths show strong preference for the outer walls of these fossils; inner walls tend to be smooth (Fig. 13G). Overgrowths are not observed on the simple tubes or on *Cloudina.*

Evidence of calcite mineralization is intriguing because field and petrographic studies show that aragonite was favored as the common marine cement in Nama environments, accreting ooids, filling neptunian dikes that cross-cut pinnacle reefs, growing among thrombolitic mesoclots in reefs, and lining primary void space in grainstones (Grant 1990; Grotzinger unpublished data). This implies that *Namacalathus,* like *Cloudina* (Grant 1990), had already evolved the physiological capacity to regulate mineral precipitation.

Paleoecology.—*Namacalathus* populations are closely associated with thrombolitic textures, but they do not appear to have participated in reefal frame construction or sediment baffling. The ''stem and cup'' morphology of the Nama fossils suggests that they were benthic organisms attached to, rather than nestling on or within, their substrate; however, most specimens are oriented horizontally and not in inferred life position (Fig. 12A).
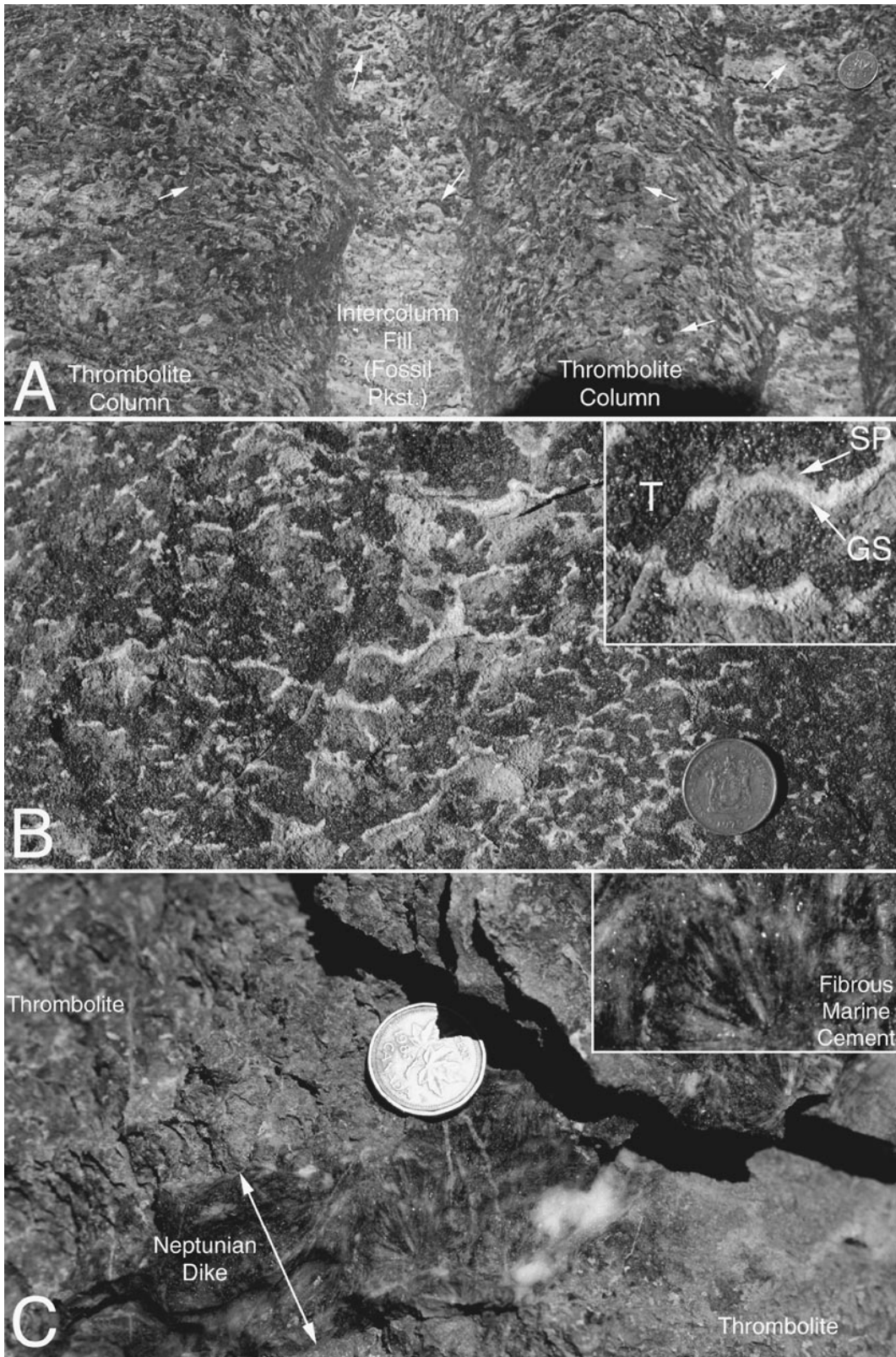
Goblets may have been attached directly to reef surfaces or anchored by an unmineralized basal holdfast to locally accumulating sediments. It is also possible, however, that *Namacalathus* individuals were attached to seaweeds or other soft-bodied macrobenthos that colonized accreting microbialites—much as living stauromedusae of the scyphozoan *Halyclystus auricula* attach to algae and sea grasses by means of disks at the ends of their exumbrellar stalks (Ruppert and Barnes 1994; Knoll personal observation). Invertebrate epibionts of sea grasses are well known from Cretaceous and Tertiary rocks, although the plants themselves are rarely preserved (Brasier 1975). More to the point, diverse and abundant macroscopic algae occur in terminal Proterozoic successions of South China (Chen et al. 1994; Steiner 1994; Xiao et al. 1998), and thallose algae grow profusely on subtidal microbialite surfaces today in places like the Bahama Banks (Feldmann and McKenzie 1998) and Shark Bay, Australia (Knoll and Grotzinger personal observations).

Whatever their mode of attachment, *Namacalathus* far outnumbered *Cloudina* and other calcified metazoans in Nama reef communities (Fig. 12B,C).

Paleobiological Interpretation.—Among metazoans, stalked radially symmetrical organisms are associated with sessile epibenthos.

$\rightarrow$

FIGURE 5.   Representative photographs of microbialites and associated textures. A, Stromatolitic thrombolite columns forming a laterally continuous biostrome at the top of the Omkyk Member, Zaris subbasin. The core of each column has a predominantly thrombolitic texture, whereas margins have better-laminated stromatolitic thrombolite texture. Columns are strongly elongate normal to the trend of the Omkyk carbonate ramp, indicating persistent high-velocity, wave-generated flows. Arrows point to goblet- and tube-shaped fossils that are abundant within the intercolumn fill sequences, but also occur within the thrombolitic texture. B, Well-preserved thrombolite texture in a pinnacle reef at the top of the Huns platform, Witputs subbasin. Reefal framework is created by dark-colored mesoclots; these create shelter pores that are partially filled by light-colored geopetal sediment and are ultimately filled by fibrous marine and later blocky burial cements. Inset shows fabric details: T = thrombolite mesoclot; GS = geopetal sediment; SP = shelter porosity filled with cement. Coin is approximately 1.2 cm in diameter. Inset shows enlargement of region near center of photograph. C, Neptunian dike transecting thrombolite mound, Driedoornvlagte bioherm, Zaris subbasin. Dike is infilled with botryoidal fibrous calcite cement, interpreted to have replaced primary aragonite. Cements fill fractures within the reef, providing evidence for early lithification of the reef. Coin is approximately 1 cm in diameter. Inset shows enlargement of region below coin.

A — Thrombolite Column, Intercolumn Fill (Fossil Pkst.), Thrombolite Column

B — T, SP, GS

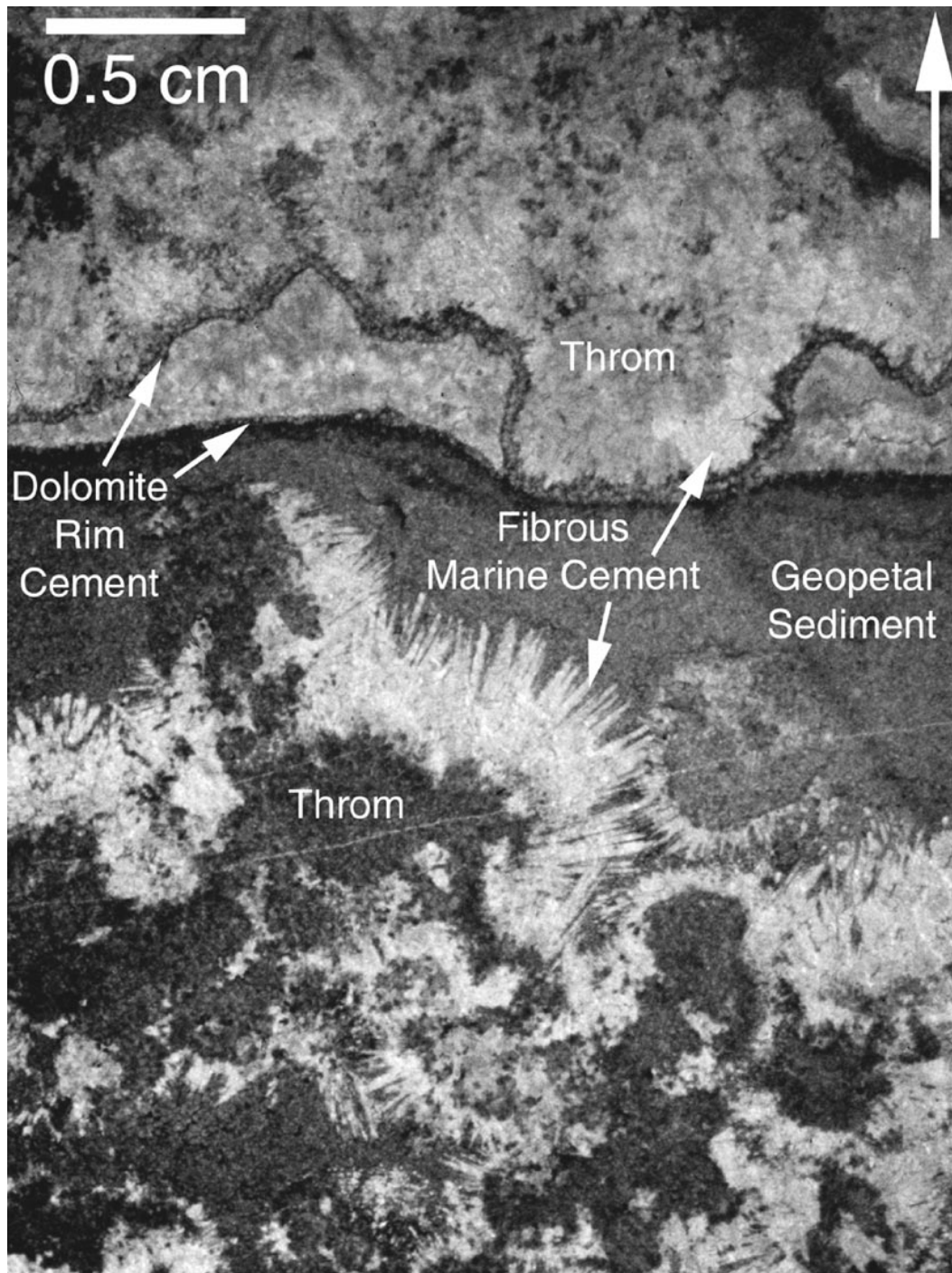C — Thrombolite, Neptunian Dike, Thrombolite, Fibrous Marine Cement

FIGURE 6.   Thin-section photomicrograph of thrombolite fabrics within a pinnacle reef at top of Huns carbonate platform, Witputs subbasin. Thrombolite mesoclots (Throm) are encrusted with a fringe of fibrous calcite (Fibrous Marine Cement) interpreted to have replaced original aragonite (note square crystal terminations). This was followed by deposition of a layer of crystal silt (Geopetal Sediment). Occlusion of remaining shelter porosity began with precipitation of an isopachous fringe of Dolomite Rim Cement, followed by a final infill of blocky calcite spar. Note that mesoclots are composed of distinct aggregates of smaller clots. These smallest fabric elements most likely are formed by the early cementation of coccoid microorganisms. Note the accumulation of Geopetal Sediment (crystal silt), which smoothes out the rugged relief created by clots and encrusting Fibrous Marine Cements.
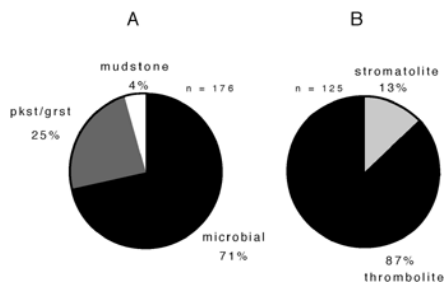
FIGURE 7. Proportional distribution of calcified fossils within broadly defined lithologic facies of the Nama Group (A) and within microbial facies of the Nama Group (B). Data were collected by recording every bed within a single measured section, and noting their facies and fossil content. If any fossils were observed, the bed was counted as ''fossiliferous'' and recorded. Results show that fossils are very strongly correlated with microbial facies in general, and with thrombolitic facies in particular. Fossils are less abundant in packstones and grainstones, which are composed principally of intraclasts and peloids, and are rare in mudstones. The simplest interpretation of this distribution is that the fossil organisms were benthic, with a strong preference for microbially colonized substrates. In addition, the preference for thrombolitic over stromatolitic substrates suggests further paleoecologic control on their distribution. See text for discussion.

Phylogenetically, goblet morphology might be expected to occur among the Porifera, the Cnidaria, or early stem branches of the Bilateria (before the evolution of strongly bilateral symmetry). *Namacalathus* could, thus, in principle be viewed as the remains of simple asconid sponges with thin body walls and a relatively large spongocoel. Such an interpretation would be consistent with reports of Ediacaran impression (Gehling and Rigby 1996), biomarker (McCaffrey et al. 1994), and spicule (Brasier et al. 1997) fossils that suggest a broader importance of this group in terminal Proterozoic communities, and, more generally, with the phylogenetic expectation that sponges should have appeared early (Nielsen et al. 1996). On the other hand, the walls of the Nama fossils contain no evidence of pores or spicules. The former could, of course, have been obliterated during diagenesis, and the latter is not conclusive insofar as not all sponges synthesize mineralized spicules. The observations are made to underscore the point that Nama goblets contain no features beyond overall shape that suggest affinities with sponges. The symmetric distribution of side holes is not easily reconciled with poriferan functional biology.

Chalice- or goblet-like morphologies can be found among the Cnidaria—for example, in hydrozoan polyps, the asexual scyphopolyps of some scyphozoans, and sessile scyphozoan stauromedusae in which exumbrellar surfaces are elongated into stalks (Ruppert and Barnes 1994). The side holes characteristic of *Namacalathus* fossils can be reconciled with a cnidarian bodyplan, especially if these holes are interpreted as diagenetic features whose persistent occurrence and regular arrangement reflect underlying biological structure. In a number of specimens, sediment within goblets is distinct in color or texture from externally encompassing sediments. The boundary between sediment types is commonly just as sharp across side holes as it is across preserved walls (see Fig. 11), suggesting that wall material once existed where holes are found today. In contrast, mixing of internal and external sediments suggests that the gap at the top of the cups was open at time of burial.

Features potentially capable of governing the positions of lateral holes include (unmineralized) tentacles at some distance from the mouth (Brusca and Brusca 1990), planuloid buds arising from surfaces of goblet-shaped scyphopolyps (e.g., *Cassiopea* [Lesh-Laurie and Suchy 1991: Fig. 59]), or radially distributed biological structures such as septa and gonads whose decay contributed to localized dissolution of wall carbonate. Viewed in this way, *Namacalathus* can be interpreted in terms of cnidarian structure and function: sessile organisms with a mouth that opened into a large gastrovascular cavity.

Other interpretations are less attractive. Stem groups to the bilaterian (or ctenophore + bilaterian [Ax 1989; Eernisse et al. 1992; Nielsen et al. 1996]) clade might have had goblet-like morphologies, but the large internal cavity characteristic of Nama specimens isn't easily incorporated into such a view.

Calcification occurs within the red, green, and, to a limited extent, brown algae, but no known living or fossil forms (Wray 1977; Fritsch 1965; Graham and Wilcox 2000) are similar in morphology to the Nama fossils. *Namacalathus* does not display the internal cel-

lular structure that is ubiquitous among calcified rhodophytes; nor is the goblet morphology of this fossil approximated by known red algae. Calcifying green algae in the orders Codiales and Dasycladales precipitate aragonite intercellularly within thalli, so that preserved skeletal carbonates include hollow molds of the complex filaments that underpin thallus morphology; no such internal structure marks the Nama fossils. Some Paleozoic dasyclads had a bulbous morphology, but their external profile reflects interlocking elements that arise from a central stalk rather than a continuous sheet of cellular material. *Namacalathus* is unlikely to be an alga.

Still less attractive are comparisons with broadly vase-shaped protists such as tintinnids, allogromid foraminifera, and testate amoebae. Known living and fossil species have volumes as much as three orders of magnitude less than those of the Nama fossils (Lee et al. 1985).

In addition to comparisons with living organisms, one can ask how *Namacalathus* compares with other fossils. The cuplike structure of *N. hermanastes* is at least broadly reminiscent of the small, radially symmetrical impressions found abundantly in some Ediacaran assemblages (e.g., Narbonne and Hofmann 1987; Sokolov 1997). It calls to mind, as well, specimens of the problematic calcareous fossil *Khatsaktia* and rare corallimorphs from Lower Cambrian carbonates in Siberia and elsewhere (Debrenne et al. 1990). The hexagonal symmetry of many *Namacalathus* specimens further recalls the triradiate symmetry characteristic of some Ediacaran organisms (e.g., *Tribrachidium* and *Albumares* [Fedonkin 1990]) and the calcareous anabaritids, tubular fossils found in uppermost Proterozoic and Lower Cambrian successions (Qian and Bengtson 1989; Bengtson et al. 1990). The weakly calci-

fied Nama fossils do not, in general, appear to be phylogenetic precursors of the diverse, skeletonized bilaterian animals found in Cambrian and younger rocks.

Evidence of Further Diversity.—Germs (1972a) described two species of *Cloudina, C. reimkeae* and *C. hartmannae. Namacalthus hermanastes* adds to the diversity of calcified Nama animals but does not exhaust it. Approximately 10% of the forms observed on thrombolitic surfaces cannot be ascribed to *Namacalathus* or *Cloudina,* and we believe that these represent one or more additional, if poorly characterized, taxa. Calcified Nama fossils certainly include additional populations of simple tubes. These fossils, which commonly show a gentle curvature, are typically 1–2 mm wide. Maximum lengths are harder to estimate because the fossils are almost always broken, but segments up to 3 cm long have been observed. Shell walls are very thin and appear to reflect carbonate impregnation of an organic matrix. At least some of the tubes are closed at the base (Fig. 14D), differentiating them from *Namacalathus* stems. Smooth walls, as seen in petrographic thin-section, further differentiate these tubes from *Cloudina* (see discussion, below). Monospecific tube assemblages occur in micritic carbonates that accumulated on level bottoms on the Nama platform.

Like other Nama fossils, the simple tubes are problematic. Functional considerations suggest that their makers were benthic organisms that lived erect on the seafloor, perhaps filter feeders analogous to if not necessarily homologous with modern fan or feather-duster polychaete (annelid) worms (Brusca and Brusca 1990). Calcareous polychaete tubes are known from limestones as old as Ordovician (Steele-Petrovich and Bolton 1998), and unmineralized polychaetes occur in the Burgess

→

FIGURE 8. Assemblage of calcified *Namacalathus* fossils within reefal and related thrombolitic horizons within the Nama Group. A, *Namacalathus* packstone illustrating a range of cross-sectional morphologies. B, Single large *Namacalathus,* over 2 cm in diameter. Note overgrowth of euhedral calcite on shell wall (see Fig. 13G for photomicrograph of similar fringe). C, Cross-sections of two *Namacalathus* fossils. The first defines a well-developed hexagon, while the second, which came to rest inside the first, is composed of three segments. D, Another specimen showing hexagonal geometry. E, Original goblet-shaped fossil described by Grotzinger et al. (1995). Note adjacent cup-shaped fossils, which also represent cross-sections of *Namacalathus.* All specimens in A–E can be explained as random sections through a single three-dimensional morphology (see text).
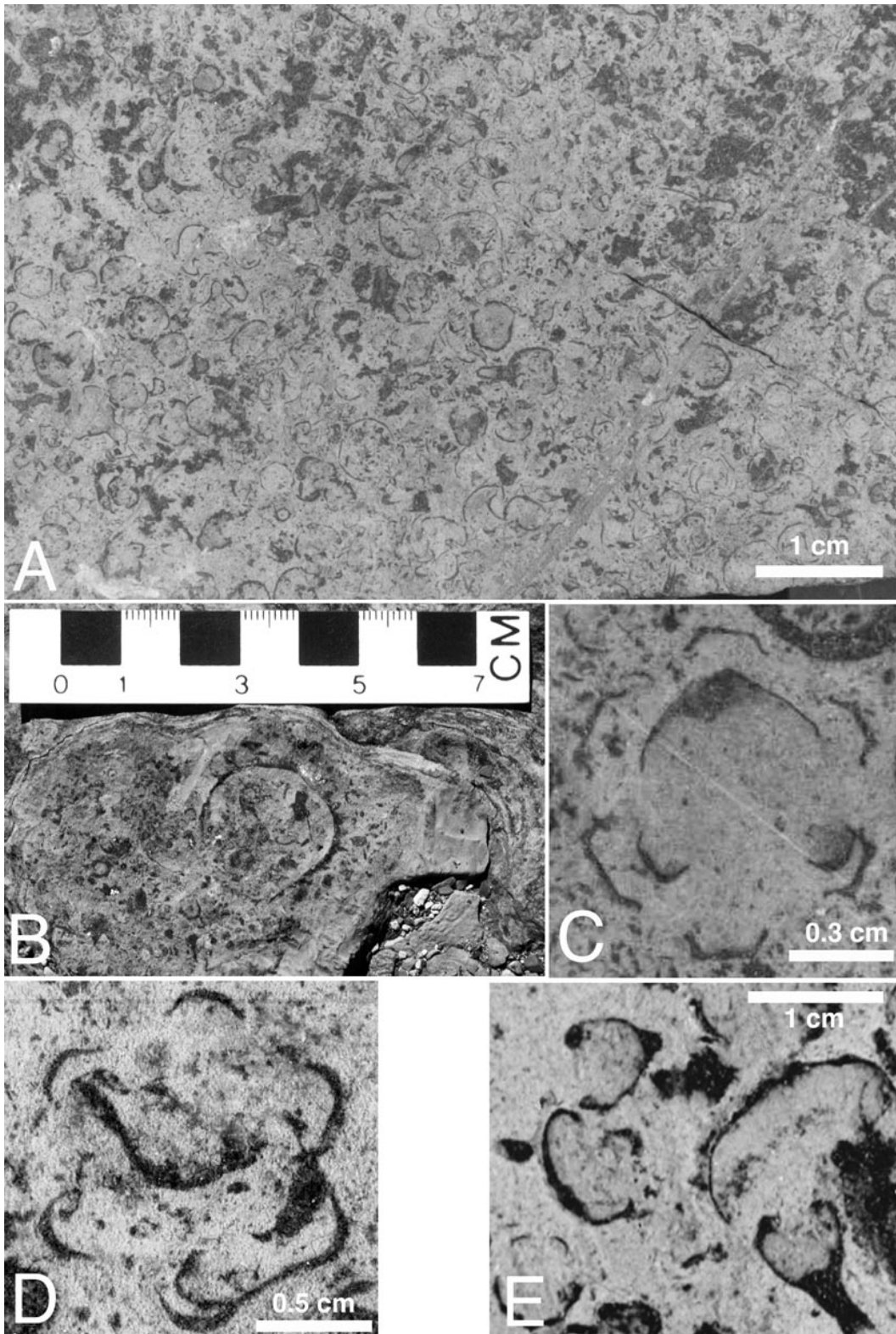
Shale and its Lower Cambrian counterparts (Conway Morris 1998).

Exceptionally preserved populations allow fresh observations of *C. riemkeae,* the smaller and lesser known of the two *Cloudina* species in Nama rocks. The highest concentrations of this taxon occur in association with a flooding surface developed atop the Driedoornvlagte bioherm. Like the larger *C. hartmannae, C. riemkeae* has been reconstructed as a series of stacked cones (see Grant 1990; Bengtson and Zhao 1992); however, primary marine cements that line a continuous inner surface emphasize that the ''cones'' are funnel-like flanges formed episodically during the growth of a cylindrical tube. The outer part of each flange diverges from the tube wall, whereas the inner part merges with the bases of earlier-formed flanges (Fig. 14A–C). Several workers (Germs 1972a; Glaessner 1976; Conway Morris et al. 1990) have noted points of structural similarity between *Cloudina* and tube-forming annelids such as the serpulid *Merceriella* (Fauvel 1923). The morphologies illustrated in Figure 14 also resemble the (unmineralized) tubes of some modern pogonophorans (Ivanov 1963), as well as diagenetically mineralized vestimentiferan worm tubes recovered from Cretaceous vent deposits in California (Little et al. 1999). (Pogonophorans and vestimentiferans are considered to nest phylogenetically within the Annelida [McHugh 1997].) Alternatively, *C. riemkeae* might be compared to the episodically accreting (unmineralized) sheaths of budding scyphozoan polyps (Werner 1967). Whatever its affinities to living organisms, *C. riemkeae* does resemble *Saarina,* organically preserved tubes from the Vendian of the Russian platform that are comparably organized (Sokolov 1997). Some Early Cambrian anabaritids also have well developed flanges (Bengtson et al. 1990; Qian and Bengtson 1989).

The Nama Group thus contains at least five taxa of calcified metazoans: *C. hartmannae* and *C. riemkeae* (Germs 1972a; Grant 1990), *N. hermanastes,* simple closed tubes, and the uncharacterized forms in reef assemblages. More taxa may be recognized in continuing work; for example, fragmental remains in skeletal packstones hint at additional diversity. In absolute terms, observed diversity is modest, but, then, only about a dozen species of canonical Ediacaran fossils have been reported from Nama sandstones (Richter 1955; Pflug 1970a,b, 1972; Germs 1972b,c; Runnegar 1992; Narbonne et al. 1997).

Globally, the Ediacaran biota contains fewer than 100 taxa (Fedonkin 1990; Runnegar 1992). Additional species of calcified metazoans have been described from terminal Proterozoic beds in Brazil (Hahn and Pflug 1985), and small mineralized fossils (foraminiferans?) have been claimed to occur in correlative units in Uruguay (Gaucher and Sprechmann 1999). Phosphatized tubes in the terminal Proterozoic Doushantuo Formation, China, may or may not be of animal origin (Li et al. 1997). Regardless of uncertainties surrounding the Uruguayan and Chinese structures, calcified fossils constitute at least five percent of known Ediacaran diversity—not very different from the proportional representation of mineralized species in the Middle Cambrian Burgess Shale (Conway Morris 1998). The confirmation that a number of Proterozoic animals were able to precipitate mineralized skeletons lends support to the hypothesis that physiological pathways integrated in skeletal biomineralization evolved early in the history of animals, if not earlier (Westbroek and Marin 1998). In consequence, the subsequent Cambrian diversification of well-skeletonized animals likely reflects increasing levels of predation rather than physiological innovation per se (Bengtson 1994).

Despite expanding a distinct taphonomic

→

FIGURE 9. Tomographic reconstructions of the calcified fossil *Namacalathus hermanastes.* First described as having a ''goblet'' shape (Grotzinger et al. 1995), the fossil has a well-defined stem that is attached to an outward flaring cup perforated by six or seven incurved holes, with an upper circular opening lined by an inward-turning lip. Partial specimens A through H are shown in inferred growth position (top) and also viewed from above (bottom). Note basal stem (or what is left of it) attached to a cup (A, C–G). The cup has six or seven holes, and these are apparent with a regular symmetry in the majority of cases. Note also the single, circular opening (or part of it) in the inferred tops of each specimen. Complete specimen I is shown from several perspectives.
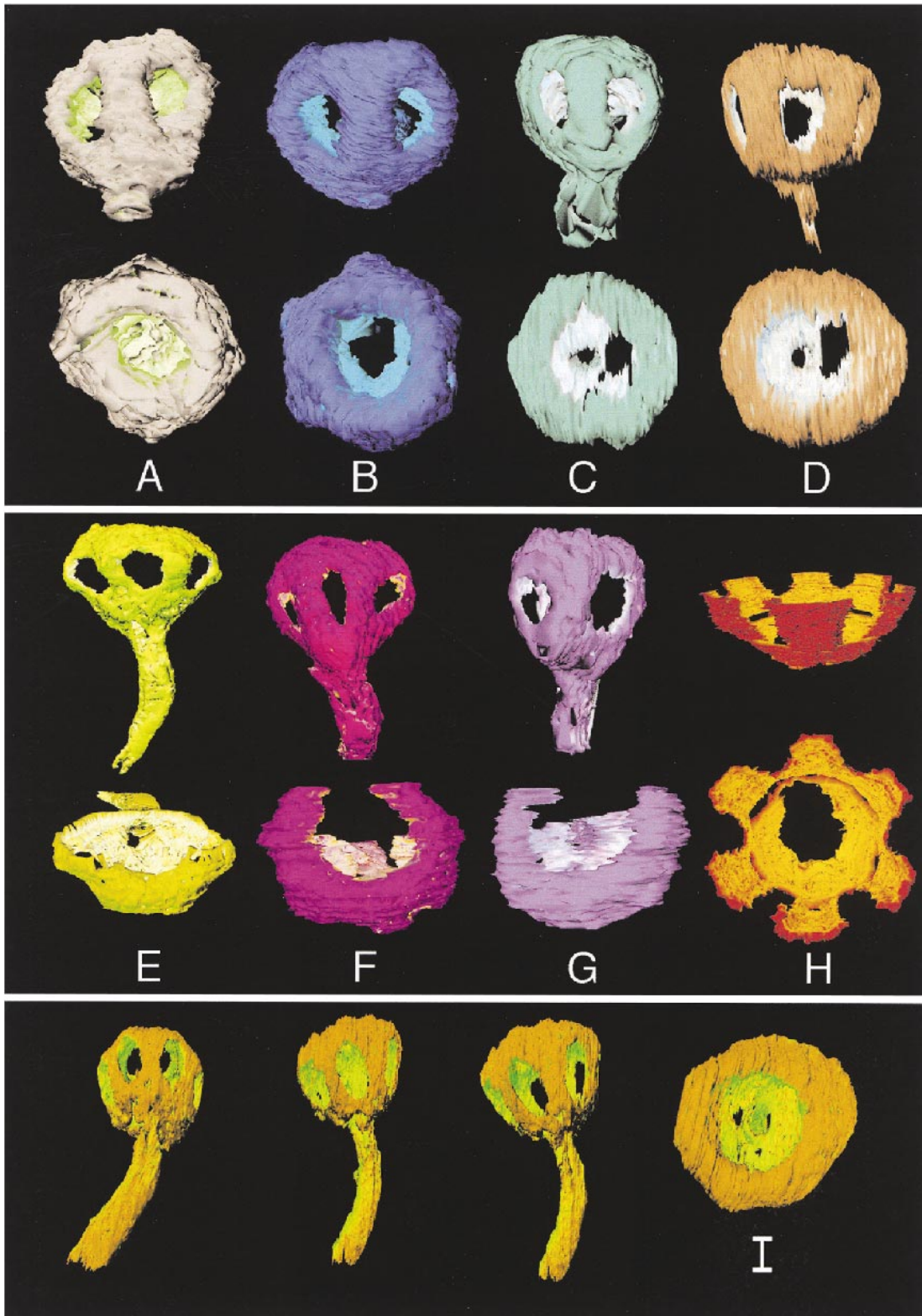
window on early animal evolution, calcified Nama fossils do not reveal Proterozoic roots for the skeletonized bilaterians that radiated across carbonate platforms in the Paleozoic Era. On the contrary, like the Ediacaran assemblages preserved in contemporaneous siliciclastic rocks, calcified Nama assemblages appear to document a distinctively Proterozoic fauna.

Systematic Paleontology

Genus *Namacalathus* n. gen.

Type Species.—*Namacalathus hermanastes* n. sp.

Diagnosis.—Centimeter-scale, chalice- or goblet-shaped fossils consisting of a calcareous wall less than 1 mm thick; a basal stem open at either end connects to a broadly spheroidal cup perforated by six or seven holes with slightly incurved margins distributed regularly around the cup periphery and separated by lateral walls; the cup contains an upper circular opening lined by an incurved lip.

Etymology.—From the Nama Group and the Greek *kalathos,* denoting a lily- or vase-shaped basket with a narrow base or, in latinized form, a wine goblet.

Namacalathus hermanastes n. sp. (Figs. 8–11)

Diagnosis.—A species of *Namacalathus* distinguished by cups 2–25 mm in maximum dimension, with aspect ratio (maximum cup diameter/cup height) of 0.8–1.5.

Description.—Goblet-shaped calcified fossils; walls flexible, ca. 100 μ thick (original wall dimensions commonly obscured by diagenetic cement growth); basal cylindrical stem, hollow and open at both ends, 1–2 mm wide and up to 30 mm long, attached to spheroidal cup; cup with maximum dimension 2–25 mm, broad circular opening at top with inward-curving lip, perforated by six to seven slightly incurved holes of similar size and shape distributed regularly about cup periphery. Specimens preserved principally by void-filling calcite, with rare preservation of primary, organic-rich wall.

Etymology.—From the Greek, *herma,* meaning sunken rock or reef, and *nastes,* meaning inhabitant.

Material.—More than 1000 specimens from biohermal carbonates of the Kuibus and Schwarzrand Subgroups, terminal Proterozoic Nama Group, Namibia.

Type Specimen.—Our understanding of *Namacalathus hermanastes* derives principally from virtual fossils modeled from serially ground surfaces. Systematic practice, however, requires that real fossils be designated as types. Accordingly, the specimen illustrated in the lower right corner of Figure 8E is designated as holotype for the species. The type specimen is to be reposited in the paleontological collections of the Museum of the Geological Survey of Namibia, as collection No. F314. Representative specimens are also housed in the Paleobotanical Collections of the Harvard University Herbaria (HUHPC No. 62989).

Type Locality.—Reefal biostrome developed at the top of the Omkyk Member, Zaris Formation, Kuibis Subgroup, exposed along the Zebra River near the boundary between Donkergange and Zebra River farms, south of Bullsport, Namibia.

$\rightarrow$

FIGURE 10. Mathematical models, based on 11 geometric parameters that capture the essential morphology of *Namacalathus hermanastes* (B and D) and cross-sections of tomographic models upon which these are based and which were used to obtain parameter values (A and C). A (from model B in Fig. 9), Cross-sections, through center of cup, showing regular holes sliced horizontally (relative to growth position) (top), and vertically through growth axis (upper-middle); and wire-frame views of circular opening at inferred top (lower-middle) and of the cup in profile (bottom). B, Mathematical model informed by the images in A. C, The same cross-sections and wire-frame diagrams for Model I in Figure 9. D, Mathematical model based upon the images in C. Specimen in A-B was collected from a locality in the Zaris subbasin; the specimen in C-D is from the Witputs subbasin. The two models are primarily distinguished by (1) the number of holes (six in the case of A-B, seven in the case of C-D); (2) the radial profile of the cup (reaching maximum diameter near the top of the cup for C-D and near the middle in the case of A-B); (3) the wall curvature (nearly flat at the cup's midheight in C-D while still slightly round in A-B); and (4) the size of the inward-turning lip that lines the cup's upper circular opening.
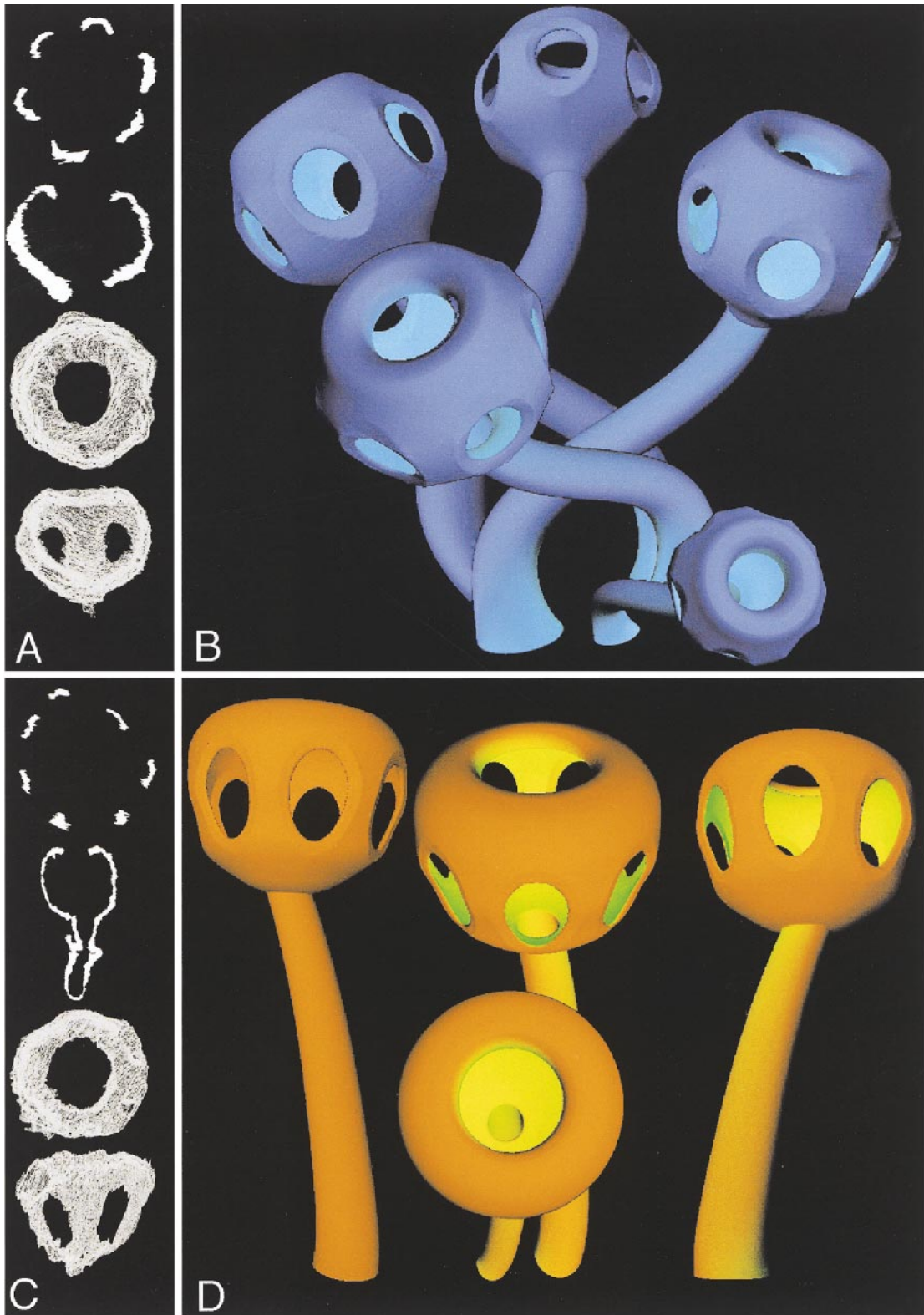
Thrombolite-Stromatolite-Metazoan Reefs

Thrombolite/invertebrate associations characterize Early Cambrian and some younger Paleozoic reefs (Soja 1994; Kruse et al. 1995; Riding and Zhuravlev 1995). Nama bioherms show that the close ecological relationship between invertebrate and microbial populations was established before the end of the Proterozoic Eon, prompting questions about the origins of this distinctive reef association.

Microbial mat populations have contributed to stromatolitic reef accretion since the Archean (Hofmann et al. 1999; Grotzinger and Knoll 1999), but bioherms characterized by thrombolitic textures are rare before the latest Proterozoic Eon (Aitken 1967). Partly on the basis of this stratigraphic distribution, Walter and Heys (1984) interpreted thrombolitic clots as ordinary stromatolitic laminae disrupted by burrowing. Kennard and James (1986), however, subsequently demonstrated that thrombolitic textures are primary, confirming the original inference of Aitken (1967). Kennard and James argued specifically that the diagnostic clotted fabric of thrombolites is generated by in-situ calcification of coccoid-dominated microbial communities. Coccoid cyanobacteria form rough, irregular mats that may, upon calcification, yield a clotted texture with only crude lamination (Hofmann 1975), and recent work supports this interpretation for some Neoproterozoic thrombolites (Turner et al. 1997). Such an interpretation, however, leaves open an important question. Mats built by coccoidal cyanobacteria are common in Paleo- and Mesoproterozoic tidal flats (Golubic and Hofmann 1976; Sergeev et al. 1995), but thrombolitic fabrics are essentially absent. How can this discrepancy be explained?

Feldmann and McKenzie (1998) have recently proposed that ancient thrombolites reflect the participation of higher algae in mat-building consortia. This inference is based on actualistic observations on the Bahama Banks, where cyanobacteria-dominated mat communities accrete well-developed laminae in intertidal environments, whereas eukaryotic communities produce poorly laminated, thrombolitic textures in open-marine subtidal environments. Coccoid spores thought to be produced by dasycladalean green algae play a particularly important role in fabric generation.

The observations of Feldmann and McKenzie (1998) are consistent with paleoenvironmental research that locates Paleozoic thrombolites in subtidal environments (Aitken 1967; Bova and Read 1987; Pratt and James 1986). They are also congruent with biostratigraphic data that bracket the expansion of thrombolites between the initial diversification of green algae and the appearance of well-skeletonized dasyclads (Wray 1977; Knoll 1992).

Observations of Nama thrombolites are also consistent with predictions of the Feldmann and McKenzie (1998) model. Nama thrombolites formed in open-marine, wave-swept environments, often associated with grainstone shoals. Well-laminated stromatolites are rare in the Nama Group, but so are intertidal facies. The best-developed Nama stromatolites form columns within a sheetlike biostromal unit at the top of the Omkyk Member (Fig. 3B,C)—a unit interpreted to have formed in a very shallow subtidal environment. Significantly, thrombolitic textures are most abundant and best developed in pinnacle reefs at the top of the Huns platform and at Driedoornvlagte. These reefs are composed of large mounds, which are rarely elongate; where elongation is developed, it is defined by a low length-to-width ratio, consistent with low current velocities in deeper-water subtidal settings. Thrombolite textures developed in this environment are similar to those found in Pa-

→

FIGURE 11.   Diverse cross-sections of *Namacalathus hermanastes* might be interpreted as different taxa (upper photos); however, virtual slices through the mathematical models shown in Figure 10 produce a diverse array of synthetic cross-sections (lower images) that can be used to estimate species richness. Most of the diverse cross-sections of calcified fossils in Nama rocks can be explained in terms of a single morphology with some minor variations. The cross-sections shown in the upper photos were obtained from 40 specimens, only two of which were used to generate tomographic reconstructions (Fig. 9E,F).

leozoic rocks (compare Fig. 5B with Fig. 2B of Kennard and James 1986).

As noted above, *Namacalathus* and other Nama metazoans lived in specific association with thrombolitic substrates, forming both reefs and level-bottom accumulations. Despite their greater abundance in reefs, these animals did not participate in any substantial way in reef building, either as framebuilders or sediment bafflers. With this in mind, it is straightforward to visualize a paleoecologic reconstruction in which the calcified organisms were loosely attached to the accreting thrombolitic substrate, much as calcisponges and green algae are in modern Bahamian thrombolites. Alternatively, *Namacalathus* may have been an epibiont attached to seaweeds or soft-bodied animals that colonized the thrombolitic substrate. Upon death or dislocation of the algal components, calcified organisms would have collapsed to the seafloor as detrital particles to be swept into the depressions between thrombolite columns and mounds, or occasionally to be trapped in random positions within accreting mats. This interpretation also provides a mechanistic basis for understanding the locally great abundance of detached, horizontally oriented fossils in thin (a few cm) beds of thrombolitic laminites that form spatially extensive sheets within deeper subtidal facies. Before the radiation of metazoan macrograzers, broad expanses of the terminal Proterozoic seafloor may have been covered by microbial-algal carpets, with calcified metazoans attached to a (tiered?) algal lawn. Animals assumed a constructional role

in bioherm accretion only with the evolution of heavily skeletonized, attached epibenthos.
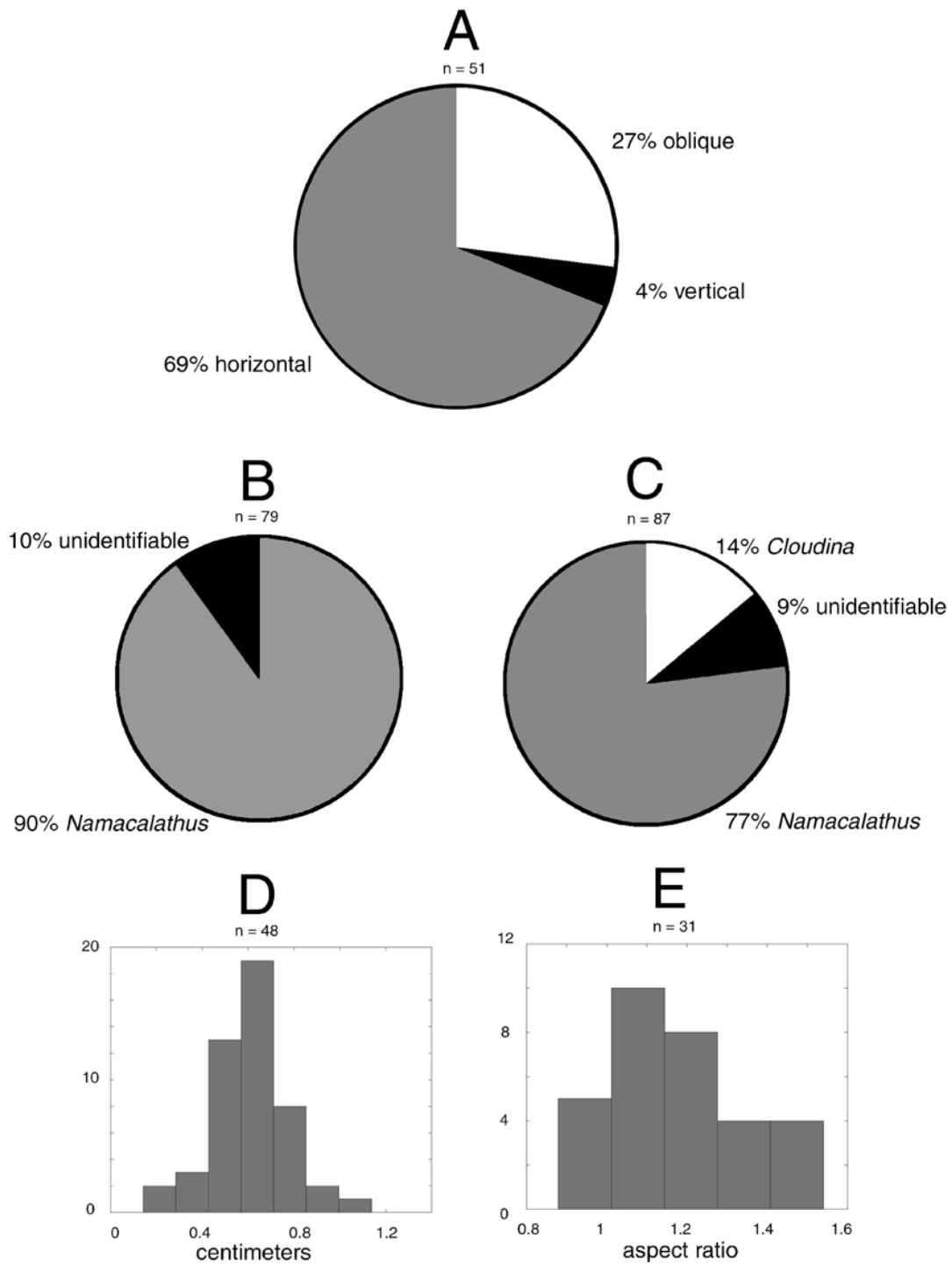
Conclusions

Nama bioherms document the emergence of a distinctive reef association. Animals that lived in the reef environment include some of the first organisms able to form skeletons by the enzymatic precipitation of $CaCO_3$ on an organic template. In important ecological and physiological respects, then, Nama bioherms and the fossils they contain foreshadow Paleozoic biology. At the same time, however, *Namacalathus hermanastes* and other calcified Nama fossils are morphologically, and perhaps phylogenetically, distinct from Paleozoic skeleton formers. At present the significance of these similarities and differences is not completely known, but continuing study of the vast and beautifully exposed carbonate accumulations of the Nama Group promises to clarify our understanding of terminal Proterozoic biology and geobiology.

Acknowledgments

$\rightarrow$

FIGURE 12.   Statistics on the orientation, diversity, and geometry of calcified fossils in the Nama Group. A, Percentage of *Namacalathus* fossils in three categories of orientation for specimens within a single sample from the Witputs subbasin. ''Vertical orientation'' describes fossils with a cross-section parallel to bedding that show the six or seven regular holes at the cup's midsection (as in Fig. 8C,D). This orientation spans approximately 22°, measured for the angle formed by the cup's symmetry axis and the bedding plane, at the cup's geometric center. ''Horizontal orientation'' describes specimens with cross-section parallel to bedding, simultaneously showing the cup's upper circular opening and the basal hole to which the stem attaches. This orientation spans an angle of approximately 25°, measured in the same way. ''Oblique orientation'' describes fossils that fit neither of the above categories; these span an angle of 43°. It follows that if there were no preferred orientation, 28% of fossils would have a vertical orientation, 24% horizontal, and 38% oblique. Instead, we find that the vast majority (69%) have a horizontal orientation. B, Percentage of fossils by type found in a sample from the Zaris subbasin. C, Percentage of fossils by type found in a sample from the Witputs subbasin. D, Size distribution of *Namacalathus* cups within a sample from the Witputs subbasin (size = average of cup diameter and height). Mean size = 0.61 cm. E, Distribution in aspect ratio (maximum cup diameter to cup height) from the same sample. Mean aspect ratio = 1.18.

A

n = 51

27% oblique

4% vertical

69% horizontal

B

n = 79

10% unidentifiable

90% *Namacalathus*

C

n = 87

14% *Cloudina*

9% unidentifiable

77% *Namacalathus*
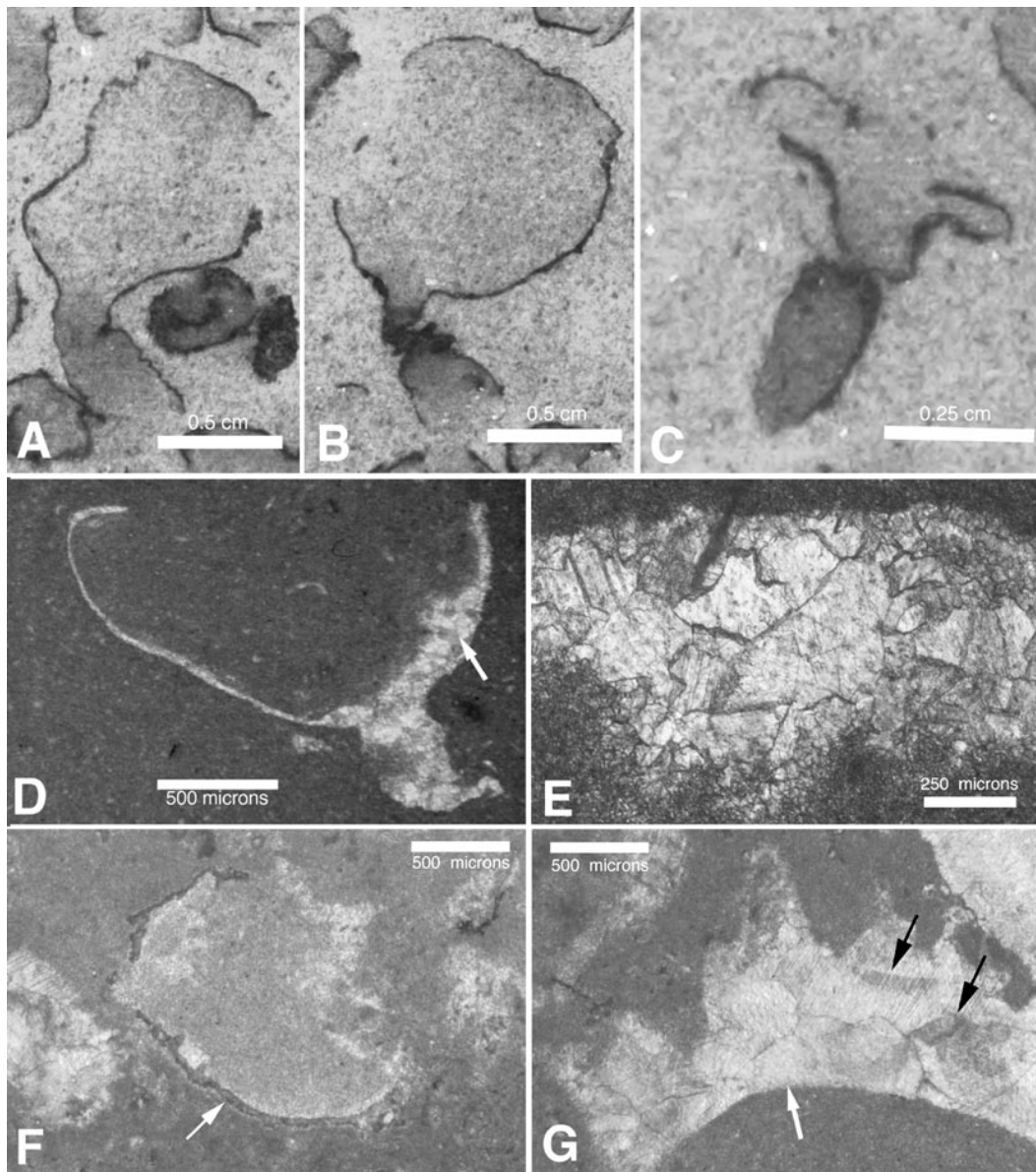
D

n = 48

centimeters

E

n = 31

aspect ratio

FIGURE 13. Taphonomic aspects of *Namacalathus*. Most of the photographs indicate the relatively flexible nature of the wall, suggesting only light mineralization at time of death. A–C, Deformational features include folds and wrinkles in walls and stems; squashed and flattened cups; cups without stems, presumably because of postmortem breakage; wall ruptures, holes, and impressions caused by adjacent objects; and disintegration of walls. D, Cross-section through a goblet-shaped fossil, illustrating replacement by void-filling calcite. Arrow points to section enlarged in Figure 13E. E, Void-filling calcite indicates decay/dissolution of primary wall. Note crystal size enlargement toward center of fossil wall. F, Rare preservation of primary shell structure (arrow) showing calcite-impregnated, dark organic matrix. In most specimens, this material has decayed/dissolved, with secondary void space filled by void-filling calcite (as in Fig. 13D,E). G, Wall of cup-shaped fossil. Note that the inner part of wall is smooth (white arrow), while the outer part is overgrown by a relatively thick layer of replacive calcite. Note crystal terminations extending out into and replacing matrix. Black arrows point to replaced intraclasts in original matrix. This suggests that nucleation and orientation of mineral overgrowths were controlled by primary crystal orientation within the fossil wall.
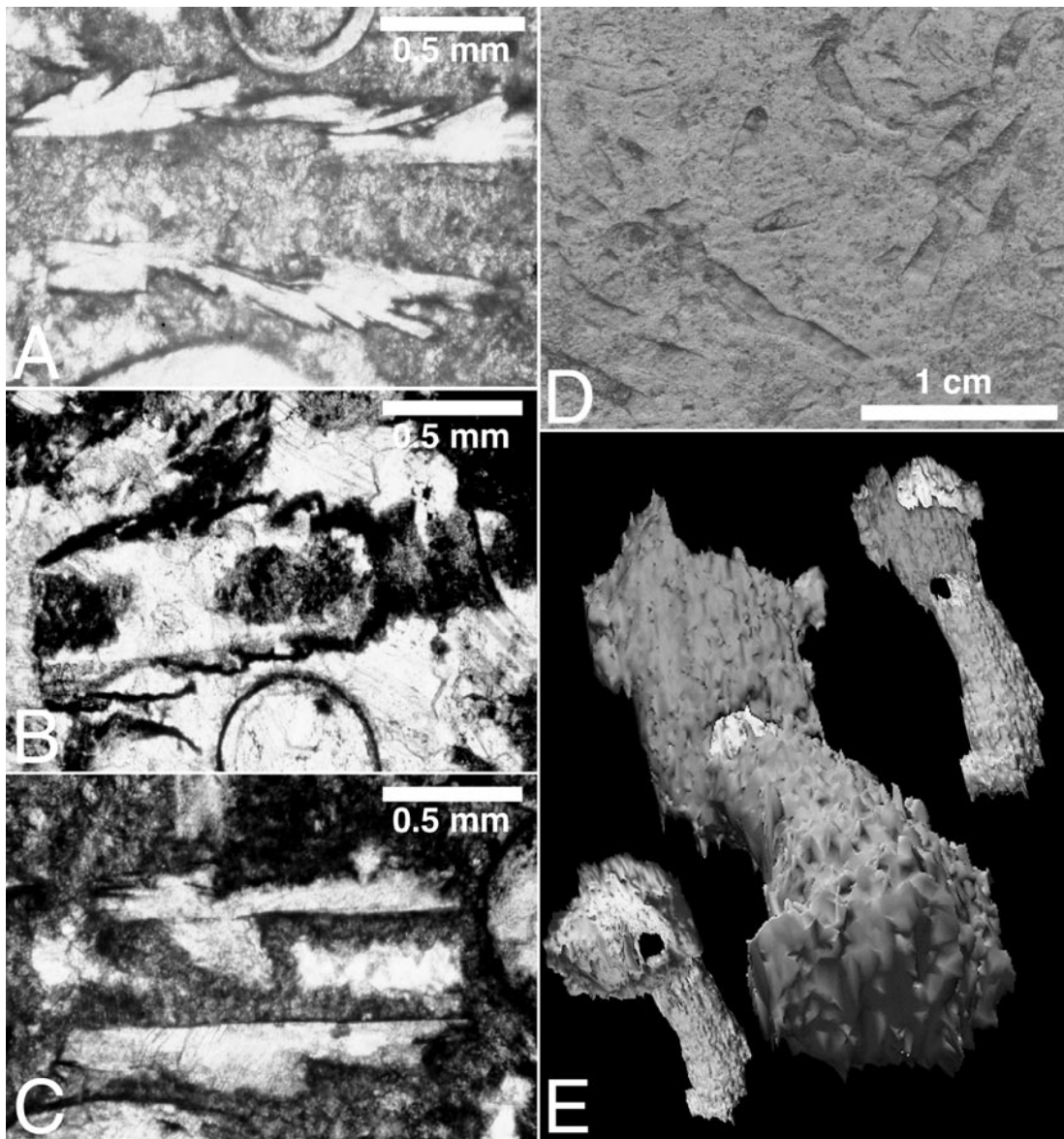
FIGURE 14. Other calcified fossils in the Nama Group. A–C, Thin-section photomicrographs of *Cloudina riemkeae* showing unusually good preservation of shell structure. In all three cases, note the straight inner wall, highlighted best in B and C, but also visible in A. A and B show external wall structure indicating *en echelon* stacking of flanges, which have largely been recrystallized in C. D, Tube-shaped fossils constituting a distinct population of shapes, distinct from both *Cloudina* and *Namacalathus*. E, Tomographic reconstruction of a tube-shaped fossil, showing its closed base and flared top.

Literature Cited

Aitken, J. D. 1967. Classification and environmental significance of cryptalgal limestones and dolomites, with illustrations from the Cambrian and Ordovician of southwestern Alberta. Journal of Sedimentary Petrology 37:1163–1178.

Ax, P. 1989. Basic phylogenetic systematization of the Metazoa. Pp. 229–245 in B. Fernholm, K. Bremer, and H. Jornvall, eds. The hierarchy of life. Elsevier, Amsterdam.

Bartley, J. K., M. Pope, A. H. Knoll, M. A. Semikhatov, and P. Yu. Petrov. 1998. A Vendian-Cambrian boundary succession from the northwestern margin of the Siberian Platform: stratigraphy, palaeontology, chemostratigraphy and correlation. Geological Magazine 135:473–494.

Bengtson, S. 1994. The advent of animal skeletons. Pp. 412–425 in S. Bengtson, ed. Early life on Earth. (Nobel Symposium No. 84.) Columbia University Press, New York.

Bengtson, S., and Y. Zhao. 1992. Predatorial borings in late Precambrian mineralized exoskeletons. Science 257:367–369.

Bengtson, S., S. Conway Morris, B. J. Cooper, P. A. Pell, and B. Runnegar. 1990. Early Cambrian fossils from South Australia. Memoirs of the Association of Australasian Palaeontologists 9:1–364.

Bova, J. P., and J. F. Read. 1987. Incipiently drowned facies within a cyclic peritidal ramp sequence, Early Ordovician Chepultepec interval, Virginia Appalachians. Geological Society of America Bulletin 98:714–727.

Brasier, M. D. 1975. An outline history of seagrass communities. Palaeontology 18:681–702.

Brasier, M., O. Green, and G. Shields. 1997. Ediacaran sponge spicule clusters from southwestern Mongolia and the origins of the Cambrian fauna. Geology 25:303–306.

Brusca, R. C., and G. J. Brusca. 1990. Invertebrates. Sinauer, Sunderland, Mass.

Cecile, M. P., and F. H. A. Campbell. 1978. Regressive stromatolite reefs and associated facies, Middle Goulburn group (Lower Proterozoic), in Kilohigok Basin, N.W.T.: an example of environmental control of stromatolite form. Bulletin of Canadian Petroleum Geology 26:237–267.

Chen, M., Z. Xiao, and X. Yuan. 1994. A new assemblage of megafossils—Miaohe biota from the upper Sinian Doushantuo Formation, Yangtze Gorges. Acta Palaeontologica Sinica 33:391–403.

Conway Morris, S., 1998. The crucible of creation: the Burgess Shale and rise of animals. Oxford University Press, Oxford.

Conway Morris, S., B. W. Mattes, and M. Chen. 1990. The early skeletal organism Cloudina: new occurrences from Oman and possibly China. American Journal of Science 290-A:245–260.

Debrenne, F., J. Lafuste, and A. Zhuravlev. 1990. Coralomorphes et spongiomorphs l'aube du Cambrien. Bulletin du Museum National d'Histoire Naturelle, 4ᵉ Série, C 12:17–39.

Eernisse, D. J., J. S. Albert, and F. E. Anderson. 1992. Annelida and Arthropoda are not sister taxa: a phylogenetic analysis of spiralian metazoan morphology. Systematic Biology 41:305–330.

Fauvel, P., 1923. Bulletin de la Société Zoologique du France 47:424.

Fedonkin, M. A. 1990. Systematic description of the Vendian metazoa. Pp. 71–120 in B. S. Sokolov and A. B. Iwanowski, eds. The Vendian System, Vol. 1. Springer, Berlin.

Feldmann, M., and J. McKenzie. 1998. Stromatolite-thrombolite associations in a modern environment, Lee Stocking Island, Bahamas. Palaios 13:201–212.

Fritsch, F. E. 1965. The structure and reproduction of the algae, Vol. I. Cambridge University Press, Cambridge.

Gaucher, C., and P. Sprechmann. 1999. Upper Vendian skeletal fauna of the Arroyo del Solidado Group, Uruguay. Beringeria 23:55–91.

Gehling, J., and J. K. Rigby. 1996. Long expected sponges from the Neoproterozoic Ediacaran fauna of South Australia. Journal of Paleontology 70:185–195.

Germs, G. J. B. 1972a. New shelly fossils from the Nama Group, South West Africa. American Journal of Science 272:752–761.
———. 1972b. The stratigraphy and paleontology of the lower Nama Group, South West Africa. Bulletin, Precambrian Research Unit 12:1–250. University of Cape Town, Cape Town.

———. 1972c. Trace fossils from the Nama Group, South West Africa. Journal of Paleontology 46:864–870.
———. 1974. The Nama Group in South West Africa and its relationship to the Pan African Geosyncline. Journal of Geology 82:301–317.
———. 1983. Implications of a sedimentary facies and depositional environmental analysis of the Nama Group in South West Africa/Namibia. In R.M. Miller, ed. Evolution of the Damara Orogen. Geological Society of South Africa Special Publication 11:89–114.

Glaessner, M. F. 1976. Early Phanerozoic annelid worms and their geological and biological significance. Journal of the Geological Society, London 132:259–275.

Golubic, S., and H. J. Hofmann. 1976. Comparison of modern and mid-Precambrian Entophysalidaceae (Cyanophyta) in stromatolitic algal mats: cell division and degradation. Journal of Paleontology 50:1074–1082.

Graham, L. E., and L. W. Wilcox. 2000. Algae. Prentice-Hall, Upper Saddle River, N. J.

Grant, S. W. F. 1990. Shell structure and distribution of Cloudina, a potential index fossil for the terminal Proterozoic. American Journal of Science 290-A:261–294.

Gresse, P. G., and G. J. B. Germs. 1993. The Nama foreland basin: sedimentation, major unconformity bounded sequences and multisided active margin advance. Precambrian Research 63:247–272.

Grotzinger, J. P. 1986. Evolution of an early Proterozoic passive margin carbonate platform, Rocknest Formation, Wopmay Orogen, Northwest Territories, Canada. Journal of Sedimentary Petrology 56:831–847.
———. 1989. Facies and evolution of Precambrian carbonate depositional systems: emergence of the modern platform archetype. In P. D. Crevello, J. L. Wilson, J. F. Sarg, and J. F. Read, eds. Controls on carbonate platform and basin development. Society of Economic Paleontologists and Mineralogists Special Publication 44:79–106.
———. In press. Facies and paleoenvironmental setting of thrombolite-stromatolite reefs, terminal Proterozoic Nama Group (ca. 550–543 Ma), central and southern Namibia. Communications of the Geological Survey of Namibia, Vol. 13 (Henno Martin Volume).

Grotzinger, J. P., and N. P. James. 2000. Carbonate sedimentation and diagenesis in the evolving Precambrian world. Society of Economic Paleontologists and Mineralogists Special Publication 65 (in press).

Grotzinger, J. P., and A. H. Knoll. 1999. Stromatolites in Precambrian carbonates: evolutionary mileposts or environmental dipsticks? Annual Review of Earth and Planetary Science 27:313–358.

Grotzinger, J. P., S. Bowring, B. Z. Saylor, and A. J. Kaufman. 1995. Biostratigraphic and geochronologic constraints on early animal evolution. Science 270:598–604.

Hahn, G., and H. D. Pflug. 1985. Die Cloudinidae n. fam., Kalk-Rohren aus dem Vendium und Unter-Kambrium. Senckenbergiana Lethaea 65:413–451.

Hoffman, P. F. 1969. Proterozoic paleocurrents and depositional history of the east arm fold belt, Great Slave Lake. Canadian Journal of Earth Science 6:441–462.

Hofmann, H. J. 1975. Stratiform Precambrian stromatolites, Belcher Islands, Canada: relations between silicified microfossils and microstructure. American Journal of Science 275:1121–1132.

Hofmann, H. J., K. Grey, A. H. Hickman, and R. I. Thorpe. 1999. Origin of 3.45 Ga coniform stromatolites in Warrawoona Group, Western Australia. Geological Society of America Bulletin 111:1256–1262.

Ivanov, A. V. 1963. Pogonophora. Translated and edited by D. B. Carlisle. Academic Press, New York.

Kennard, J. M., and N. P. James. 1986. Thrombolites and stro-

matolites: two distinct types of microbial structures. Palaios 1:492–503.

Knoll, A. H. 1992. The early evolution of eukaryotes: a geological perspective. Science 256:622–627.

Kruse, P. D., A Yu. Zhuravlev, and N. P. James. 1995. Primordial metazoan-calcimicrobial reefs: Tommotian (Early Cambrian) of the Siberian Platform. Palaios 10:291–321.

Lee, J. J., S. H. Hutner, and E. C. Bovee, eds. 1985. An illustrated guide to the Protozoa. Society of Protozoologists, Lawrence Kans.

Lesh-Laurie, G. E., and P. E. Suchy. 1991. Cnidaria: Scyphozoa and Cubozoa. Pp. 185–266 in F. W. Harrison and J. A. Westfall, eds. Microscopic anatomy of invertebrates, Vol. 2. Placozoa, Porifera, Cnidaria, and Ctenophora. Wiley-Liss, New York.

Li, G., Y.-s. Xue, and C.-m. Zhou. 1997. Late Proterozoic tubular fossils from the Doushnatuo Formation of Weng'an, Guizhou, China. Palaeoworld 7(1997):29–37.

Little, C. T. S., R. J. Herrington, R. M. Haymon, and T. Danelian. 1999. Early Jurassic hydrothermal vent community from the Franciscan Complex, San Rafael mountains, California. Geology 27:167–170.

Martin, H. 1965. The Precambrian geology of South West Africa and Namaqualand. Rustica, Wynberg, South Africa.

McCaffrey, M. A., J. M. Moldowan, P. A. Lipton, R. E. Summons, K. E. Peters, A. Jeganathan, and D. S. Watt. 1994. Paleoenvironmental implications of novel C_{30} steranes in Precambrian to Cenozoic age petroleum and bitumen. Geochimica et Cosmochimica Acta 58:529–532.

McHugh, D. 1997. Molecular evidence that echiurans and pogonophorans are derived annelids. Proceedings of the National Academy of Sciences USA 94:8006–8009.

Miller, R. M. 1983. The Pan-African Damara Orogen of South West Africa/Namibia. Pp. In R. M. Miller, ed. Evolution of the Damara Orogen. Geological Society of South Africa Special Publication 11:431–515.

Narbonne, G. M., and H. J. Hofmann. 1987. Ediacaran biota of the Wernecke Mountains, Yukon, Canada. Palaeontology 30:647–676.

Narbonne, G. M., B. Z. Saylor, and J. P. Grotzinger. 1997. The youngest Ediacaran fossils from southern Africa. Journal of Paleontology 71:953–967.

Nielsen, C., N. Scharff, and D. Eibye-Jacobsen. 1996. Cladistic analysis of the animal kingdom. Biological Journal of the Linnean Society 57:385–410.

Pflug, H. D. 1970a. Zur fauna der Nama-Schichten in Südwest Afrika. I. Pteridinia, Bau und systematische Zugehorigkeit. Palaeontographica, Abteilung A 134:226–262.

———. 1970b. Zur fauna der Nama-Schichten in Südwest Afrika. II. Rangidae, Bau und systematische Zugehorigkeit. Palaeontographica, Abteilung A 135:198–231.

———. 1972. Zur fauna der Nama-Schichten in Südwest Afrika. II. Erniettomorpha, Bau und systematische Zugehorigkeit. Palaeontographica, Abteilung A 139:134–170.

Pratt, B., and N. P. James. 1986. The St. George Group (Lower Ordovician) of western Newfoundland: tidal flat island model for carbonate sedimentation in shallow epeiric seas. Sedimentology 33:313–343.

Qian, Y., and S. Bengtson. 1989. Palaeontology and biostratigraphy of the Early Cambrian Meishuchunian Stage in Yunnan Province, South China. Fossils and Strata, 24:1–156.

Richter, R., 1955. Die Altesten Fossilen Süd-Afrikas. Senckenbergiana Lethaea 36:243–289.

Riding, R., and A. Yu. Zhuravlev. 1995. Structure and diversity of oldest sponge-microbe reefs: Lower Cambrian, Aldan River, Siberia. Geology 23:649–652.

Runnegar, B. N. 1992. Proterozoic fossils of soft-bodied metazoans (Ediacaran faunas). Pp. 999–1007 in J. W. Schopf and C. Klein, eds. The Proterozoic biosphere: a multidisciplinary study. Cambridge University Press, Cambridge.

Ruppert, E. E., and R. D. Barnes. 1994. Invertebrate zoology, 6th ed. Saunders College Publishing, Fort Worth.

Saylor, B. Z., and J. P. Grotzinger. 1996. Reconstruction of important Proterozoic-Cambrian boundary exposures through the recognition of thrust deformation in the Nama Group of southern Namibia. Communications of the Geological Survey of Namibia 11:1–12.

Saylor, B. Z., J. P. Grotzinger, and G. J. B. Germs. 1995. Sequence stratigraphy and sedimentology of the Neoproterozoic Kuibis and Schwarzrand Subgroups (Nama Group), Southwest Namibia. Precambrian Research 73:153–171.

Saylor, B. Z., A. J. Kaufman, J. P. Grotzinger, and F. Urban. 1998. A composite reference section for terminal Proterozoic strata of southern Namibia. Journal of Sedimentary Research 66:1178–1195.

Sergeev, V. N., A. H. Knoll, and J. P. Grotzinzger. 1995. Paleobiology of the Mesoproterozoic Billyakh Group, Anabar Uplift, northern Siberia. Paleontological Society Memoir 39:1–37.

Smith, O. A. 1998. Terminal Proterozoic carbonate platform development: stratigraphy and sedimentology of the Kuibis Subgroup (ca. 550–548 Ma), Northern Nama Basin, Namibia. M.S. thesis. Massachusetts Institute of Technology, Cambridge.

Soja, C. M. 1994. Significance of Silurian stromatolite-sphinctozoan reefs. Geology 22:355–358.

Sokolov, B. S., 1997. Essays on the advent of the Vendian System. KMK Scientific, Moscow. [In Russian.]

Soreghan, G. S., and K. A. Giles. 1999. Facies character and stratal responses to accommodation in Pennsylvanian bioherms, western Orogrande Basin, New Mexico. Journal of Sedimentary Research 69:893–908.

Steele-Petrovich, H. M., and T. E. Bolton. 1998. Morphology and paleoecology of a primitive mound-forming tubicolous polychaete from the Ordovician of the Ottawa Valley, Canada. Palaeontology 41:125–145.

Steiner, M. 1994. Die neoproterozoischen Megaalgen Südchinas. Berliner Geowissenschaftliche, Abhandlungen E 15:1–146.

Turner, E. C., G. M. Narbonne, and N. P. James. 1993. Neoproterozoic reef microstructures from the Little Dal Group, northwestern Canada. Geology 3:259–262.

Turner, E. C., N. P. James, and G. M. Narbonne. 1997. Growth dynamics of Neoproterozoic calcimicrobial reefs, Mackenzie Mountains, northwest Canada. Journal of Sedimentary Petrology 67:437–450.

Turner, E. C., G. M. Narbonne, and N. P. James. 2000. Framework composition of early Neoproterozoic calcimicrobial reefs and associated microbialites, Mackenzie Mountains, N. W. T. In J. P. Grotzinger and N. P. James, eds. Carbonate sedimentation and diagenesis in the evolving Precambrian world. Society of Economic Paleontologists and Mineralogists Special Publication 65 (in press).

Walter, M. R., and G. R. Heys. 1984. Links between the rise of the metazoa and the decline of stromatolites. Precambrian Research 29:149–174.

Watters, W. A. 2000. Digital reconstruction of fossil morphologies, Nama Group, Namibia. M. S. thesis. Massachusetts Institute of Technology, Cambridge.

Watters, W. A., and J. P. Grotzinger. In press. Digital reconstruction of calcified early metazoans, terminal proterozoic Nama Group, Namibia. Paleobiology 27.

Werner, B., 1967. Morphologie, Systematik, und Lebensgeschichte von Stephenoscyphus (Scyphozoa Coronatae) sowie seine Bedeutung für die Evolution der Scyphozoa. Zoologischer Anzeiger 30(Suppl.):297–319.

Westbroek, P., and Marin, F. 1998. A marriage of bone and nacre. Nature 392:861–862.

Wray, J. L. 1977. Calcareous algae. Elsevier, Amsterdam.

Xiao, S., A. H. Knoll, and X. Yuan. 1998. Morphological reconstruction of Miaohephyton bifurcatum, a possible brown alga from the Neoproterozoic Doushantuo Formation, South China. Journal of Paleontology 72:1072–1086.